



UNIVERSITY OF LEEDS

This is a repository copy of *Microchemical characterization of placer gold grains from the Meyos-Essabikoula area, Ntem complex, southern Cameroon*.

White Rose Research Online URL for this paper:
<http://eprints.whiterose.ac.uk/140090/>

Version: Accepted Version

Article:

Dongmo, FWN, Chapman, RJ, Bolarinwa, AT et al. (3 more authors) (2019) Microchemical characterization of placer gold grains from the Meyos-Essabikoula area, Ntem complex, southern Cameroon. *Journal of African Earth Sciences*, 151. pp. 189-201. ISSN 1464-343X

<https://doi.org/10.1016/j.jafrearsci.2018.12.006>

Crown Copyright © 2018 Published by Elsevier Ltd. This manuscript version is made available under the CC-BY-NC-ND 4.0 license
<http://creativecommons.org/licenses/by-nc-nd/4.0/>.

Reuse

This article is distributed under the terms of the Creative Commons Attribution-NonCommercial-NoDerivs (CC BY-NC-ND) licence. This licence only allows you to download this work and share it with others as long as you credit the authors, but you can't change the article in any way or use it commercially. More information and the full terms of the licence here: <https://creativecommons.org/licenses/>

Takedown

If you consider content in White Rose Research Online to be in breach of UK law, please notify us by emailing eprints@whiterose.ac.uk including the URL of the record and the reason for the withdrawal request.

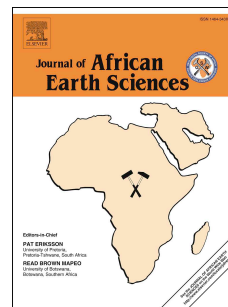


eprints@whiterose.ac.uk
<https://eprints.whiterose.ac.uk/>

Accepted Manuscript

Microchemical characterization of placer gold grains from the Meyos-Essabikoula area, Ntem complex, southern Cameroon

Franck Wilfried Nguimatsia Dongmo, Robert John Chapman, Anthony Temidayo Bolarinwa, Rose Fouateu Yongue, David A. Banks, Jerry Olugbenga Olajide-Kayode



PII: S1464-343X(18)30374-1

DOI: <https://doi.org/10.1016/j.jafrearsci.2018.12.006>

Reference: AES 3388

To appear in: *Journal of African Earth Sciences*

Received Date: 7 August 2018

Revised Date: 9 December 2018

Accepted Date: 11 December 2018

Please cite this article as: Nguimatsia Dongmo, F.W., Chapman, R.J., Bolarinwa, A.T., Yongue, R.F., Banks, D.A., Olajide-Kayode, J.O., Microchemical characterization of placer gold grains from the Meyos-Essabikoula area, Ntem complex, southern Cameroon, *Journal of African Earth Sciences* (2019), doi: <https://doi.org/10.1016/j.jafrearsci.2018.12.006>.

This is a PDF file of an unedited manuscript that has been accepted for publication. As a service to our customers we are providing this early version of the manuscript. The manuscript will undergo copyediting, typesetting, and review of the resulting proof before it is published in its final form. Please note that during the production process errors may be discovered which could affect the content, and all legal disclaimers that apply to the journal pertain.

Graphical Abstract

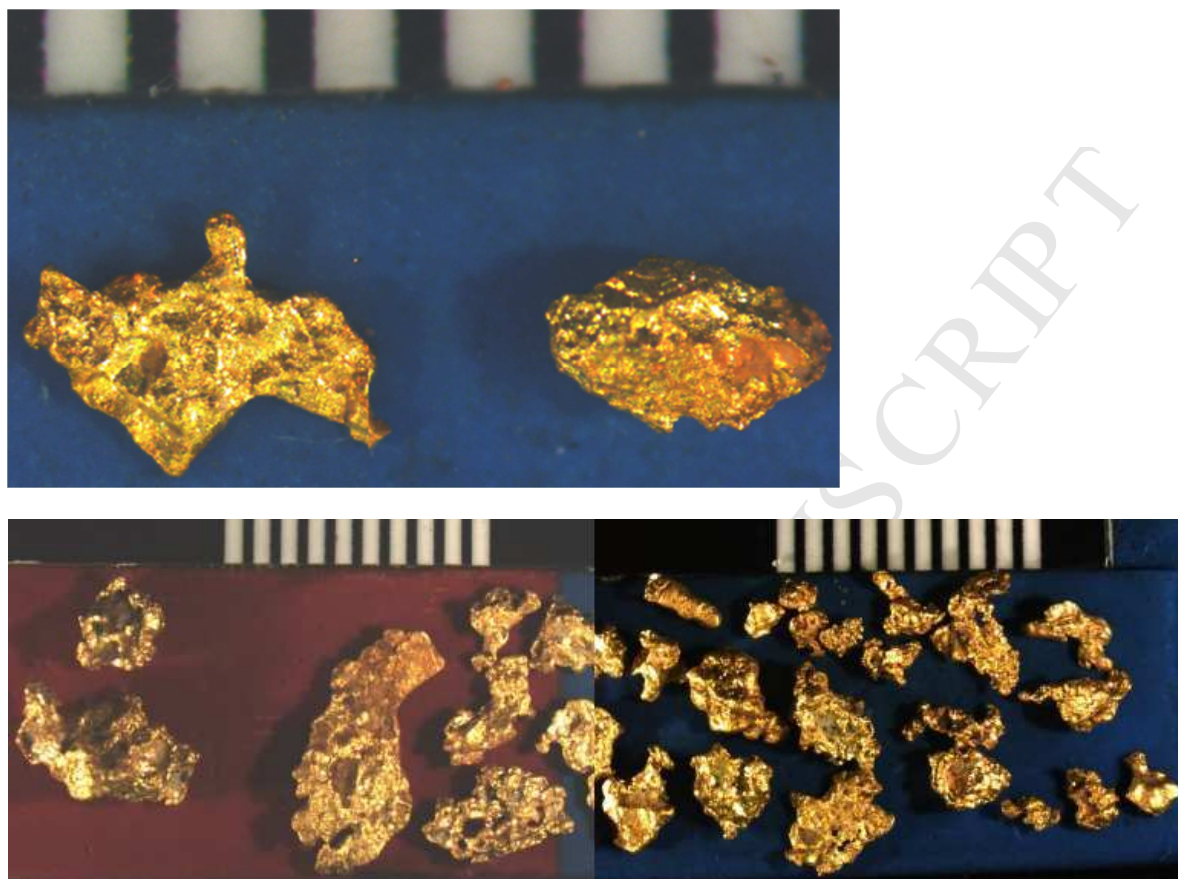


Fig.6: - Angular eluvial gold grains (Samples G8, G9, and G10). Scale bar is in mm.

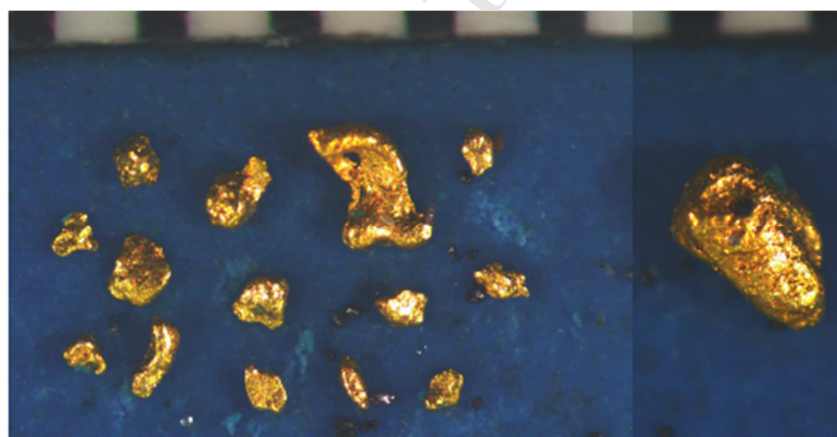


Fig.7: rounded to elongate alluvial gold grains from Nkolmedoum. The general outline of these grains is regular and surface topography tends to be smooth (Scale bar in mm).

Microchemical characterization of placer gold grains from the Meyos-Essabikoula area, Ntem complex, Southern Cameroon

Franck Wilfried Nguimatsia Dongmo^{1, 2*}, Robert John Chapman³, Anthony Temidayo Bolarinwa¹, Rose Fouateu Yongue², David A. Banks³, Jerry Olugbenga Olajide-Kayode¹

¹ Department of Geosciences, Pan African University, Life and Earth Sciences Institute (PAULESI), University of Ibadan, Ibadan, Nigeria

² Department of Earth Sciences, University of Yaounde 1, Yaounde, Cameroon

³ Ores and Mineralization Group School of Earth and Environment, University of Leeds, UK

Abstract

Gold occurs as a native metal, usually containing silver, and in some cases mercury, copper, and palladium. It may also occur as inclusions within sulfur-rich minerals, such as pyrite and arsenopyrite. The style and variety of gold mineralization is influenced by the geological setting, chemistry of the ore fluids, and the nature of their interactions with rocks. Gold grains liberated from bedrock into surficial sediments during weathering and erosion are chemically stable and may be characterized according to their mineralogy: i.e the alloy composition and suite of mineral inclusions revealed within polished sections, characteristics faithful to gold from the hypogene source. This approach has been applied to placer gold grains from the Meyos-Essabikoula area, Cameroon, where the source of gold is not yet confirmed due to poor outcrop exposure.

A total of 221 alluvial gold grains from 10 sites, tributaries of Sing and Bivele River over the Ntem Complex have been studied using Electron Probe Micro-Analysis (EMPA) to determine the concentration of minor alloying metals, (notably Au, Ag, Cu, and Hg) and Scanning Electron Microscopy (SEM) in order to evaluate the assemblage of mineral inclusions within the gold. Most of the grains are sub-rounded with pitted surfaces and inclusions of pyrrhotite, acanthite, and chalcopyrite were observed. The grains are Au-Ag alloys ranging from 54.4-99.8 wt% Au, 0.1-48.4 wt% Ag, 0.1-0.8 wt% Hg and 0-0.3 wt% Cu. The presence of Fe oxide (magnetite) inclusions containing Cr and V (to around 5 wt %) has not been reported elsewhere and suggests a strong interaction between hot reducing ore fluids and local mafic lithologies.

Keywords: Microchemical characterization, Placer gold, Alluvial and eluvial sediments. Gold morphology, Meyos-Essabikoula area, Ntem complex.

35 1. Introduction

36

37 The Meyos Essabikoula area is located within the Ntem Complex of southern Cameroon,
38 which represents the north-western part of the Congo Craton in Central Africa (Maurizot *et*
39 *al.*, 1986; Nédélec *et al.*, 1990; Goodwin, 1991). This is part of Archean terranes bearing
40 Archean lode gold deposits in Africa (Foster and Piper, 1993). The area comprises of the
41 Archean Ntem Unit to the southeast and the Paleoproterozoic Nyong Unit to the northwest.
42 Mineral exploration, in the last decade, within the southern district of Cameroon focused on
43 this area because of the abundant and widespread occurrences of placer gold, which supports
44 extensive artisanal mining. Exploration has identified a wide range of placer gold deposits,
45 however much work is needed to constrain the gold reserves in the area and their sources.

46 Recent studies show that the source(s) of the primary gold in south Cameroon is largely
47 unknown (Suh *et al.*, 2006; Omang *et al.*, 2015). This is due to several factors, including the
48 dearth of literature on primary gold mineralisation in the area, lack of adequate outcrops for
49 detailed mapping and sampling, and thick lateritic cover, which makes the geochemical
50 signature of underlying mineralization in soils difficult to determine in regional geochemical
51 surveys.

52

53 In cases such as this, valuable information regarding the origins of gold can be obtained from
54 the study of the microchemical signature of detrital gold grains. Grains of native gold are
55 chemically stable within most environments on the Earth's surface, and thus gold grains
56 liberated from the hypogene ore are normally unchanged on passing from bedrock into
57 surficial sediments as a result of weathering and erosion. They may be characterized
58 according to both their alloy composition and the suite of minerals present as inclusions. This
59 approach permits identification of populations of placer gold grains derived from different
60 sources often through correlation of assemblages of mineral inclusions with specific alloy
61 compositions (Chapman *et al.*, 2009; Chapman *et al.*, 2016; McLenaghan and Cabri, 2011;
62 Hancock and Thorne, 2011; Moles *et al.*, 2013, Omang *et al.*, 2015). The technique has been
63 applied to facilitate both local and regional analyses of the variation in gold signature and
64 relationship to host lithology (Naden *et al.*, 1994; Leake *et al.*, 1997; Chapman *et al.*, 2000a b;
65 Omang *et al.*, 2015); used as a tool in the exploration process (Potter and Styles 2003); and to
66 identify broad differences in signatures of gold from specific styles of mineralization
67 (Chapman *et al.*, 2017a, b). Using this approach in Cameroon, Omang *et al.*, (2015) suggested
68 an ultramafic source rock for the Nyong gold grains while the Lom grains were likely derived

69 from hydrothermal quartz veins. The overall morphology of gold grains reflects their
70 transport history, with characteristics inherited from the hypogene setting evident in the
71 populations derived for the eluvial environment. Several studies have shown the evolution of
72 the grain morphology of gold particles as a function of the distance travelled from the source
73 (Knight *et al* 1999a,b; Townley *et al.* 2003, Crawford, 2007). However, there are no general
74 criteria by which distance to the source may be accurately estimated in all sedimentary
75 environments. The present study focuses on the microchemical signature of alluvial gold
76 grains from the Meyos-Essabikoula area with a view to illuminating the nature and location of
77 potential primary source(s).

78

79 **2. Geographical and geological setting**

80 The Meyos-Essabikoula study area is located in Southern Cameroon, about 32 km west of the
81 city of Sangmelima. The area is characterized by a continuous chain of topographic highs and
82 deeply incised valleys. The area lies within longitude 11°38' E - 11°48' E and latitude 2°52' N
83 - 2°58' N (Fig.1). It is an integral part of Southern Cameroon, represented topographically by
84 the Ebolowa 4 c and 4d maps at a scale of 1:50000. The Meyos-Essabikoula area lies at the
85 transition between the continental equatorial climate and the equatorial monsoon climate with
86 an annual precipitation of 1672.2 mm/yr and an average temperature of 24 °C. The Meyos-
87 Essabikoula area is located within the Ntem Complex at the northern part of Congo craton
88 (Fig. 2). The Meyos-Essabikoula area is drained by rivers Abolo, Bivele and Sing, and their
89 tributaries. These water bodies form a vast dendritic network of streams flowing in the SSE-
90 NNW, SE-NW, N-S directions.

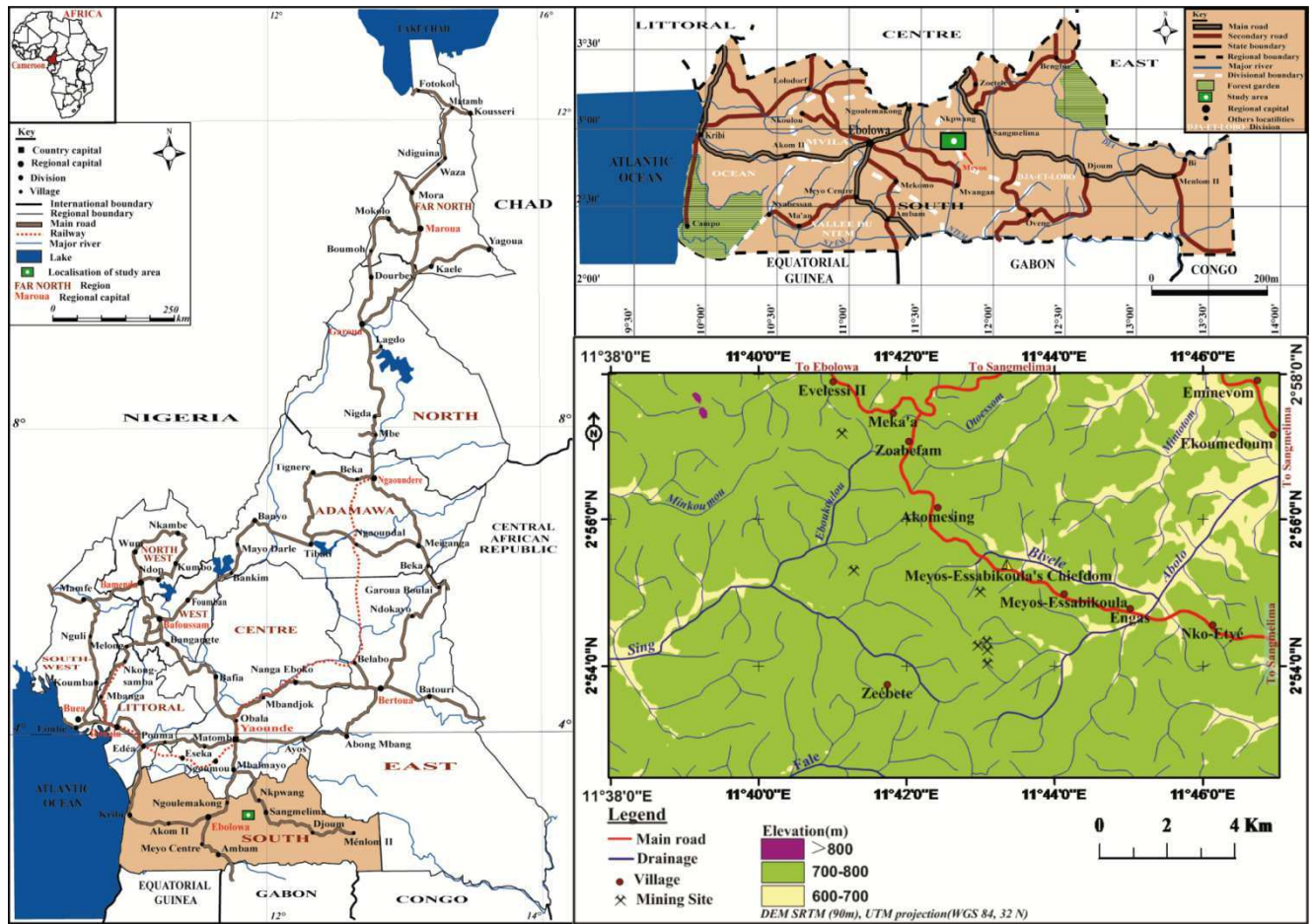
91

92 The Ntem Complex represents the north-western part of the Archaean Congo craton in
93 Central Africa (Clifford *et al.*, 1970; Cahen *et al.*, 1976; Bessoles and Trompette, 1980) and is
94 very well exposed in southern Cameroon (Rocci, 1965; Maurizot *et al.*, 1986; Goodwin,
95 1991). It is limited to the north by a major thrust that marks the contact with the Pan-African
96 orogenic belt (Yaounde group) and is composed of various rock types, with rocks of the
97 tonalite-trondhjemite-granodiorite (TTG) suite constituting the greater part (Nedelec *et al.*,
98 1990). Three main rock types, the charnockitic suite, granodioritic suite and the tonalitic suite
99 constitute the TTG unit. The tonalitic suite (Nedelec *et al.*, 1990) is exposed to the north and
100 is strongly mylonitized and retrogressed along the fault boundary with the Pan-African
101 orogenic belt. The granodioritic suite forms distinct massifs within the dominantly
102 charnockitic rocks.

103 The S0 structural surface is basically NW–SE in the charnockitic suite, NNE–SSW to almost
104 E–W in the tonalitic suite and E–W to WNW–ESE in granodiorites, indicating structural
105 discordances and suggesting a polyphase structural set-up in the Sangmelima TTG (Shang,
106 2001). Furthermore, charnockitic xenoliths occur in granodioritic and tonalitic massifs.
107 Exposures of supracrustal rocks (banded iron formations and sillimanite-bearing
108 paragneisses) that represent remnants of greenstone belts form xenoliths in TTG rocks (Nsifa
109 *et al.*, 1993). Late- to post-tectonic granitoid and syenites with alkaline affinity intrude the
110 TTG (Kornprobst *et al.*, 1976; Nedelec, 1990; Tchameni, 1997; Tchameni *et al.*, 2000, 2001;
111 Shang, 2001; Shang *et al.*, 2001a, b), and clearly postdate the major crustal forming episode.
112 Doleritic dykes of Eburnean (2.1Ga) age (Toteu *et al.*, 1994; Vicat *et al.*, 1996) represent the
113 last magmatic activity in the Ntem complex.

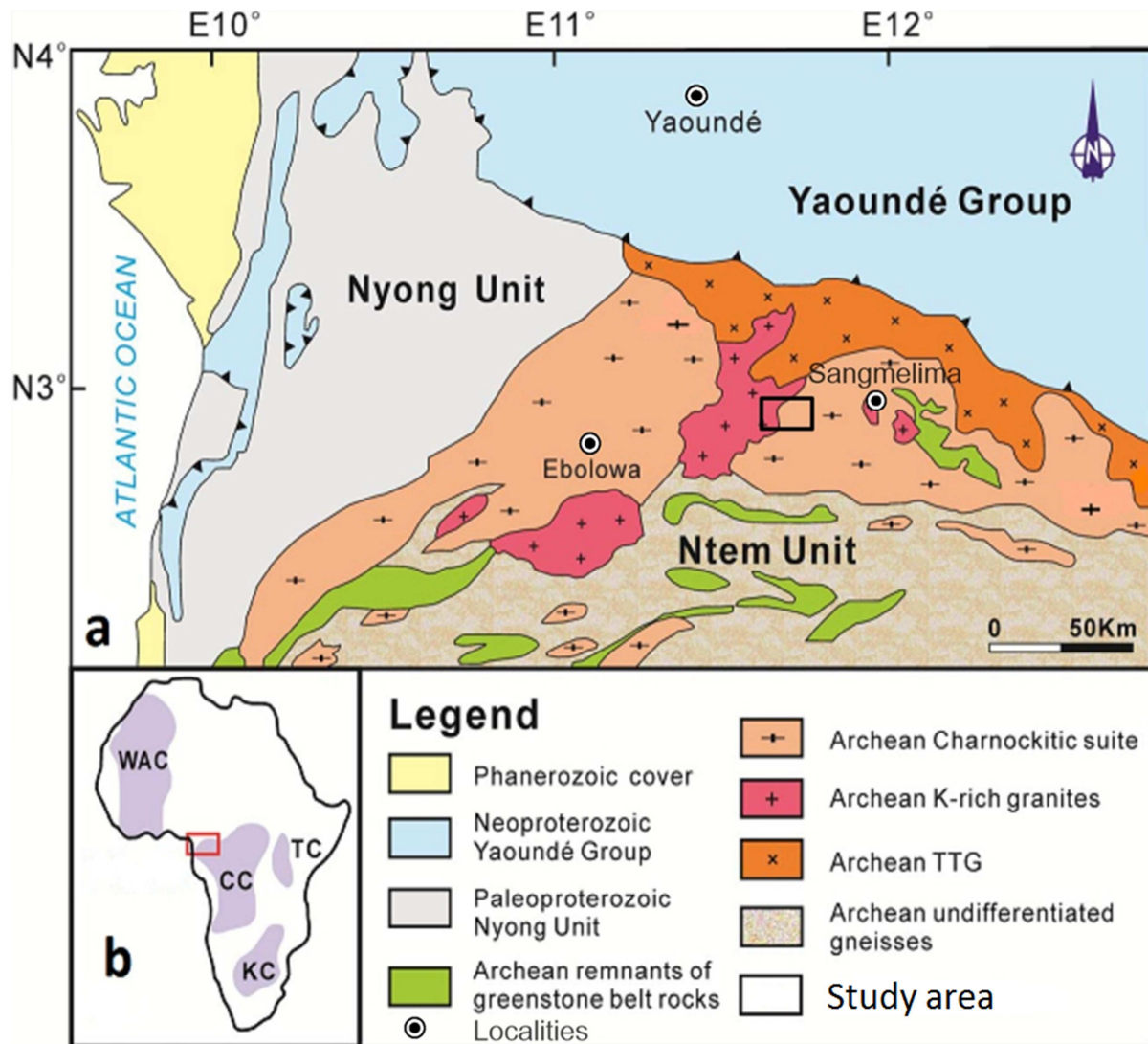
114
115 Structural studies suggest two major episodes of deformation in this geological domain. The
116 first deformation episode is characterized by vertical foliation, stretching and vertical
117 lineation and isoclinal folds. These structural elements could mark the diapiric emplacement
118 of the granitoids (Shang, 2001a; Tchameni *et al.*, 2001). The second major tectono-thermal
119 event is marked by the development of sinistral shear planes trending north-south to N45E,
120 and partial melting of charnockitic and tonalitic members of the TTG suite and the
121 greenstones, described as post-Archaean and post-charnockitic migmatization by Nsifa and
122 Riou (1990). Although the timing of this second tectono-thermal event is not well known,
123 Rb–Sr whole-rock data from Lasserre and Soba (1976) suggest that this event could have
124 occurred during the Eburnean orogeny. Toteu *et al.* (1994) dated the peak of this
125 metamorphism at about 2050Ma, using U–Pb zircon data on metamorphic rocks from the
126 Nyong series.

127 In the Meyos-Essabikoula area, the rock types are orthogneiss, amphibolites, quartzites,
128 granites, tonalite–trondhjemite–granodiorite (TTG), charnockites and quartz veins (Fig. 3).
129 Gold exploration in this area is artisanal, with no available published data on the nature of
130 gold deposition and petrogenesis.



131
 132
 133
 134
 135
 136
 137
 138
 139
 140

Fig.1: Location map of Meyos Essabikoula showing the road map of Cameroon with an inset of the map of Africa (top left), the road map of the South Region of Cameroon (top right) and the road map of Meyos Essabikoula, showing artisanal mining sites.



141

142

143 (Fig.2): a-Geological sketch map of southwestern Cameroon (modified after Maurizot *et al.*,144 1986; Tchameni *et al.*, 2010); b- showing the major Precambrian units and WAC: West145 African Craton; CC: Congo Craton; TC: Tanzanian Craton; KC: Kapvaal Craton.) (In Li *et*146 *al.*, 2016).

147

148

149

150

151

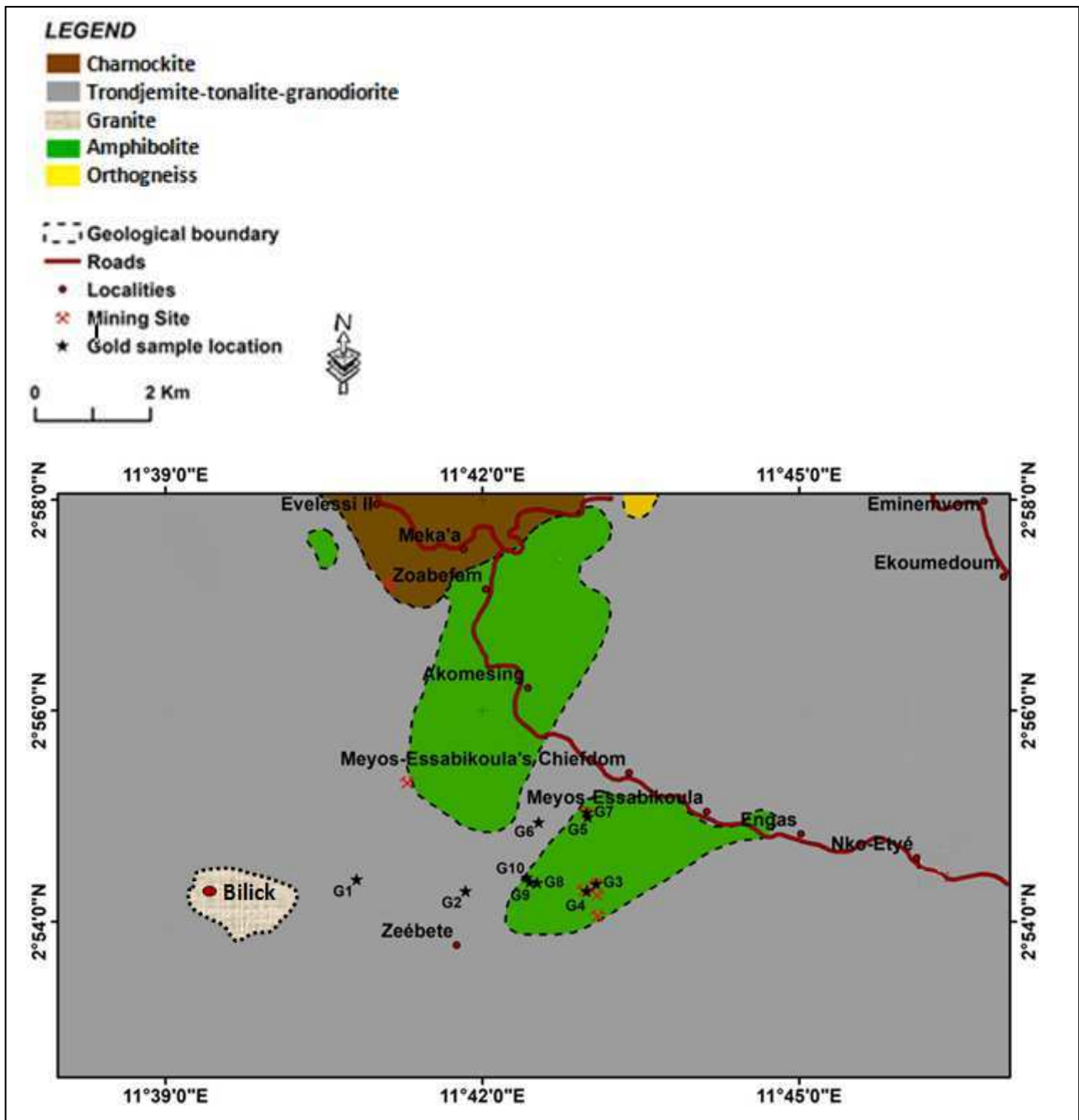
152

153

154

155

156



157
 158 Fig.3: Sketch geological map of study area, showing the distribution of rock out crops and
 159 placer gold occurrences.
 160

161
 162
 163
 164
 165
 166

167 3. Methodology

168 Sampling sites were chosen on the basis of their proximity to artisanal workings or the
169 opportunity to dig pits to the bedrock interface. Gold grains samples used in this study were
170 collected from 10 sites on tributaries of the Sing and Bivele rivers (Fig. 5) over the Ntem
171 Complex. Details of the locations and grain microchemistry of samples used in the present
172 study are presented in Table 1.

173 Gold grains were collected by hand feeding gravel into a gravity-fed sluice (Fig. 4A).
174 Auriferous gravel was collected from different types of environment: active placer mining
175 areas, previously mined areas, river spits (e.g. Fig 4B), stream beds and unmined natural
176 stream environments. The heavy mineral concentrate from each locality was hand-panned to
177 separate the gold grains.

178 The grains were photographed to record their morphological characteristics prior to mounting
179 according to size, setting in epoxy resin and polishing as described in Chapman *et al.*,
180 (2000a). Analysis was undertaken as described by Chapman *et al.* (2017a). The alloy
181 composition was determined for Au, Ag, Cu, and Hg using a Joel 8320 Super probe at the
182 University of Leeds. Inclusions were identified using the EDS facility of an FEI Quanta 650
183 FEG ESEM SEM. Some inclusions were analysed using the EDS facility of the SEM to
184 generate the semi-quantitative measurement of Cr in Fe oxide.

185 The Ag content of a population of placer gold grains is generally the first parameter studied
186 when establishing a microchemical signature, even though ultimately it may not prove the
187 most useful in determining the source style of mineralization (e.g. Chapman *et al.* 2017a,b).
188 The use of increasing Ag vs cumulative percentile plots has become a standard methodology
189 for comparing the range of Ag values of individual grains present within populations of
190 different sizes. This approach permits identification of compositional sub-populations, which
191 may be compared between localities to establish different gold types present in different
192 areas. Where detectable, Hg and Cu contents are used as additional discriminants in
193 establishing microchemical signatures, however in the present study the values of Hg are
194 almost all below the limit of detection, and Hg is not considered further.

195
196 Approaches to the characterization of mineral inclusion suites vary according to the amount
197 of data available which is, in turn, a consequence of overall abundance and population size.
198 Various studies have utilized triangular diagrams indicating relative abundance of mineral
199 classes within different assemblages (Chapman *et al.*, 2000a), although these have the
200 disadvantage of ignoring the significance of specific minerals whose presence may be

201 informative. Spider diagrams, which depict the relative abundance of different minerals
202 alleviate this issue but quickly become difficult to interpret when more than 3 or 4
203 assemblages are superimposed on the same diagram (Chapman *et al.* 2017b). In the present
204 study, inclusions were extremely scarce, but nevertheless, mineral speciation provides an
205 informative avenue of study.



228 Fig.4: (A) Methodology of collection of gold grains. (B) Example of an excavated pit at
229 Gatan locality.

230
231
232
233
234
235
236
237
238
239
240
241
242
243
244
245
246
247
248
249
250
251
252
253
254
255
256
257
258
259
260
261
262
263
264

4. Results

4.1 Gold grain morphology

Based on morphological characteristics, shape, outline, surface, associated primary crystal imprints, mineral inclusions and flatness index, two main gold grains groups were determined. The first group (Group 1) is represented by gold grains recovered from the eluvial (localities G8 and G9 (Fig. 6). Their angular and rough nature with adhering quartz and crystal imprints indicates minimal or no fluvial travel.

The second group of grains comprises rounded to oval particles, and in many cases slightly elongated shapes (Fig. 7). The outline is relatively regular and surface topography tends to be smooth. Primary mineral imprints are diffuse and associated minerals consist only of iron oxides (rare) and clay coatings. Impact and groove marks are common.

4.2 Gold alloy composition

4.2.1 Silver (Ag)

The silver contents of all sample populations are presented in Figure 8a which shows some clustering of plots with outliers (G1 G8 and G4). The other plots in figure 8 have been constructed to more clearly show the relationship between samples from localities which are adjacent or possibly related by drainage. Some of these samples contain a relatively small number of gold grains (<15) and in these cases, it is not generally possible to draw strong conclusions from the data sets. Nevertheless figure 8b shows that gold from the adjacent sites of G5, G6 and G7 yield a similar range of Ag values, whereas sample G1, which is geographically separate, comprises mainly very low Ag alloy. Samples G3 and G4 exhibit the same range of Ag alloy between 0 and around 5% and also a similar range of higher Ag alloy, although this feature is more pronounced in the gold from G4. The two eluvial samples from Nkoul Medoum, (G8 and G9) show the narrowest predominant range of Ag contents, but the two curves are not coincident. The nearby placer sample of G10 shows features of both, as does sample G2 collected approximately 1.5 km downstream.

265 Table1: Description of sample sites and general information concerning gold grains recovered
 266

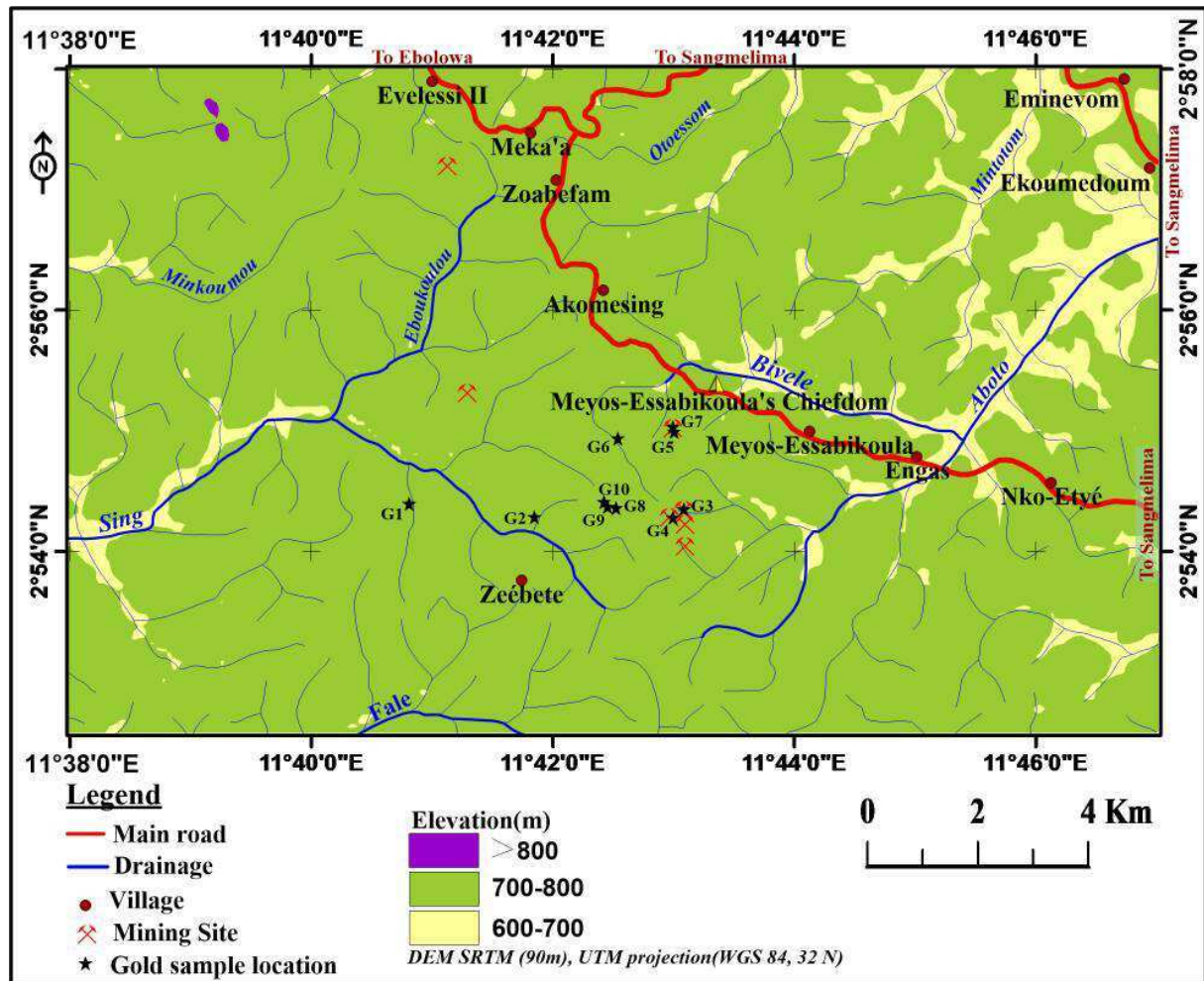
Sample No./ Locality	Coordinates	Au%		Ag%		Hg%		Cu %		Sample description
		Range	Mean	Range	Mean	Range	Mean	Range	Mean	
G1 Bilick (n=08)	2°54'24.2" 11°40'48.6" 705m	88.78- 99.56	97.41	0.06- 11.19	2.10	0.14- 0.26	0.20	0.03- 0.34	0.16	Alluvial samples obtained from a first-tier stream, which is a tributary of the River Sing. Samples were obtained at 0.6m depth from pits. The course of the stream was diverted to allow digging of the pit.
G2 Bilick (n=10)	2°54'17.6" 11°41'50.6" 702m	85.42- 99.75	93.88	0.27- 40.71	6.17	0.08- 0.33	0.21	0.03- 0.14	0.08	
G3 Zalom (n=18)	2°54'21.6" 11°43'4.8" 707m	73.77- 99.29	92.31	0.40- 26.39	7.62	0.06- 0.36	0.19	0.01- 0.19	0.08	Alluvial samples obtained from a first-tier stream which is also a tributary of the River Bivele. Samples were obtained at 0.6m depth from pits. The course of the stream was diverted to allow digging of the pit.
G4 Gatan (n=30)	2°54'17.5" 11°42'59.3" 718m	50.45- 99.59	89.76	0.31- 48.36	13.14	0.06- 0.83	0.20	0.00- 0.28	0.06	
G5 Gatan (n=12)	2°54'59.8" 11°42'59.9" 698 m	87.93- 99.44	95.32	0.39- 11.74	4.58	0.13- 0.29	0.22	0.02- 0.19	0.10	Alluvial samples from a mine pit dug in a valley. The wetland is within the catchment of River Bivele.
G6 Gatan (n=09)	2°54'56.6" 11°42'32.0" 706m	74.77 99.68	94.03	0.29 24.85	5.87	0.15 0.30	0.23	0.00 0.27	0.10	
G7 Gatan (n=04)	2°55'02.2" 11°42'59.4" 725m	73.60- 98.38	90.91	0.63- 27.34	9.24	0.11- 0.23	0.17	0.00- 0.10	0.05	Eluvial sample taken from exposed soil profile. This area is also drained by River Sing.
G8 Nkolmedoum (n=09)	2° 54' 22.3" 11° 42' 31.2" 712m	81.71- 97.41	90.51	4.43- 19.96	10.68	0.09- 0.32	0.19	0.00- 0.09	0.04	
G9 Nkolmedoum (n=25)	2° 54' 22.7" 11° 42' 27.0" 712m	56.79- 98.51	92.96	0.85- 42.53	6.50	0.07- 0.26	0.18	0.01- 0.14	0.08	Eluvial gold grains from a slope in Nkolmedoum area. This area is downslope from the Nkolmedoum swamp
G10 Nkolmedoum (n=99)	2° 54' 25.2" 11°42'25.2" 712m	52.87- 99.32	90.52	0.14- 47.24	9.16	0.05- 0.37	0.20	0.00- 0.27	0.08	
Total (221)										

267

268 n = Number of grains

269

270



271

272

273 Figure: 5: Sample location in relation to the tributaries of the Sing and Bivele Rivers

274 G1, G2: Bilick ; G3 : Zalom; G4, G5,G6,G7: Gatan; G8,G9,G10: Nkolmedoum

275

276

277

278

279

280

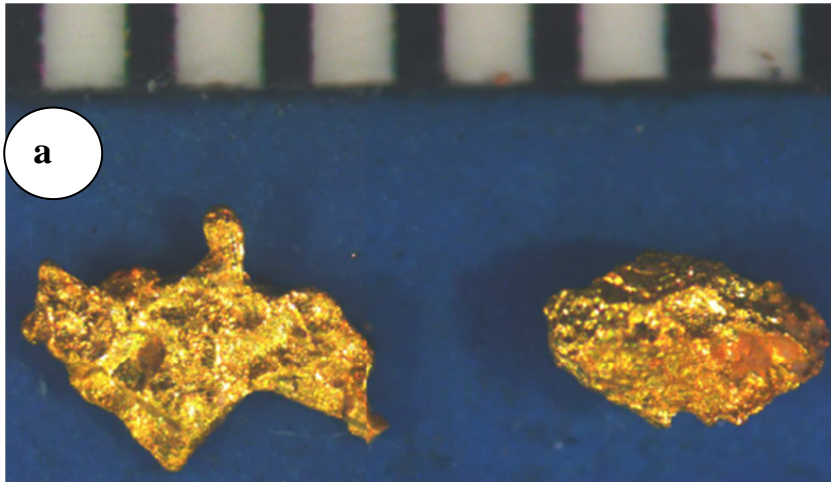
281

282

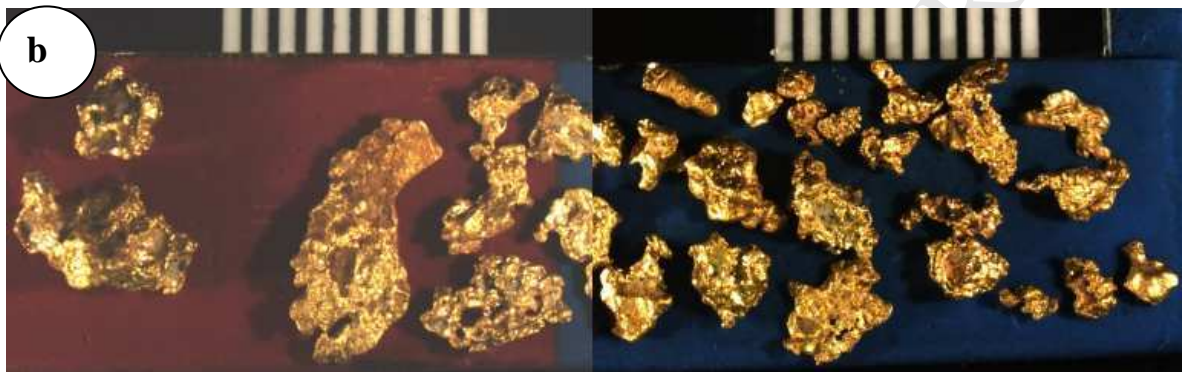
283

284

285



286

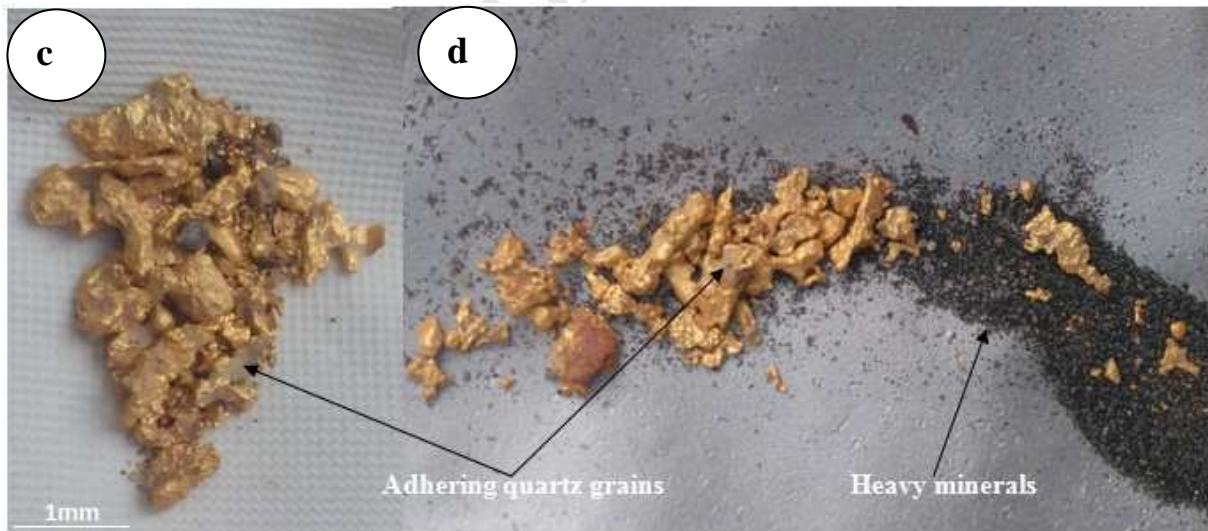


287

288

289 Fig.6 (a and b): Group 1- Angular eluvial gold grains (Samples G8, G9, and G10). Scale bar
 290 is in mm.

291



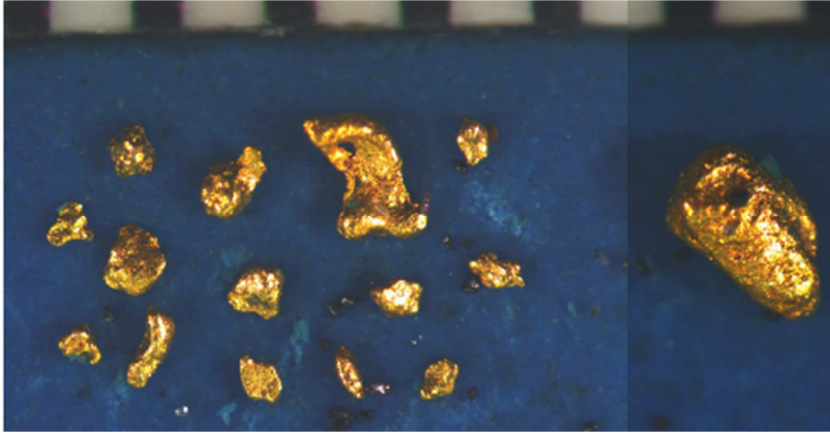
292

293 Fig.6 (c and d): Gold grains recovered from G8 and G9 localities captured immediately after
 294 panning showing adhering quartz grains and associated heavy minerals.

295

296

297



298

299

300 Fig.7: Group 2- rounded to elongate alluvial gold grains from Nkolmedoum. The general
301 outline of these grains is regular and surface topography tends to be smooth (Scale bar in
302 mm).

303

304

305

306

307

308

309

310

311

312

313

314

315

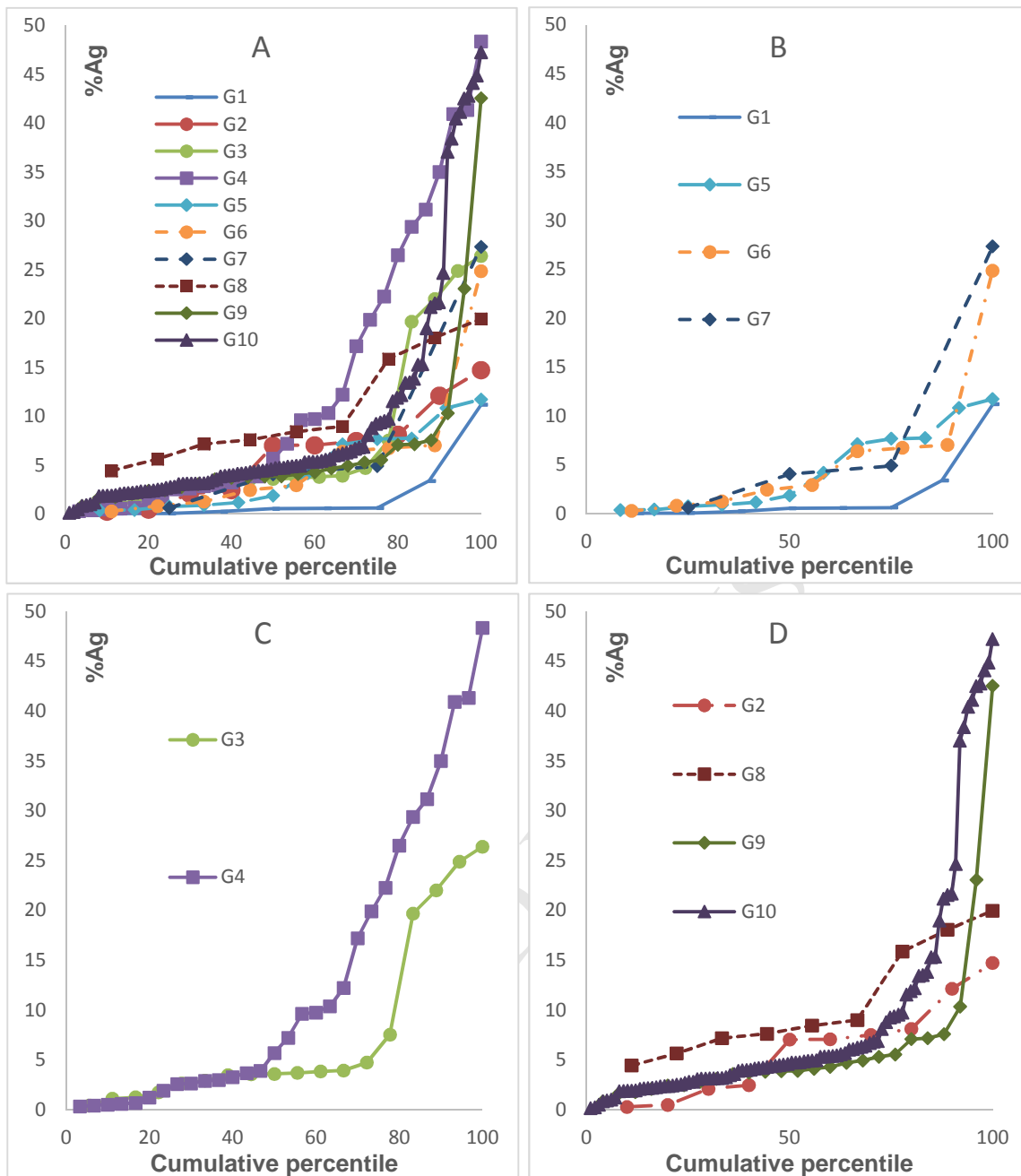
316

317

318

319

320



321

322 Fig. 8: Silver content of populations of gold grains from the study area: (A) comparison of
 323 signatures from all populations studied;(B): Comparison of signatures from adjacent placer
 324 localities, plus G1;(C): Comparison of the signatures of gold from adjacent placer localities
 325 G3 and G4;(D): comparison of silver contents of eluvial populations G8 and G9 with the
 326 adjacent placer population (G10) and a more distal placer sample (G2).

327

328

329

330

331 **Table 2:** Summary of the microchemical signature of all gold grains in which inclusions were
 332 identified
 333

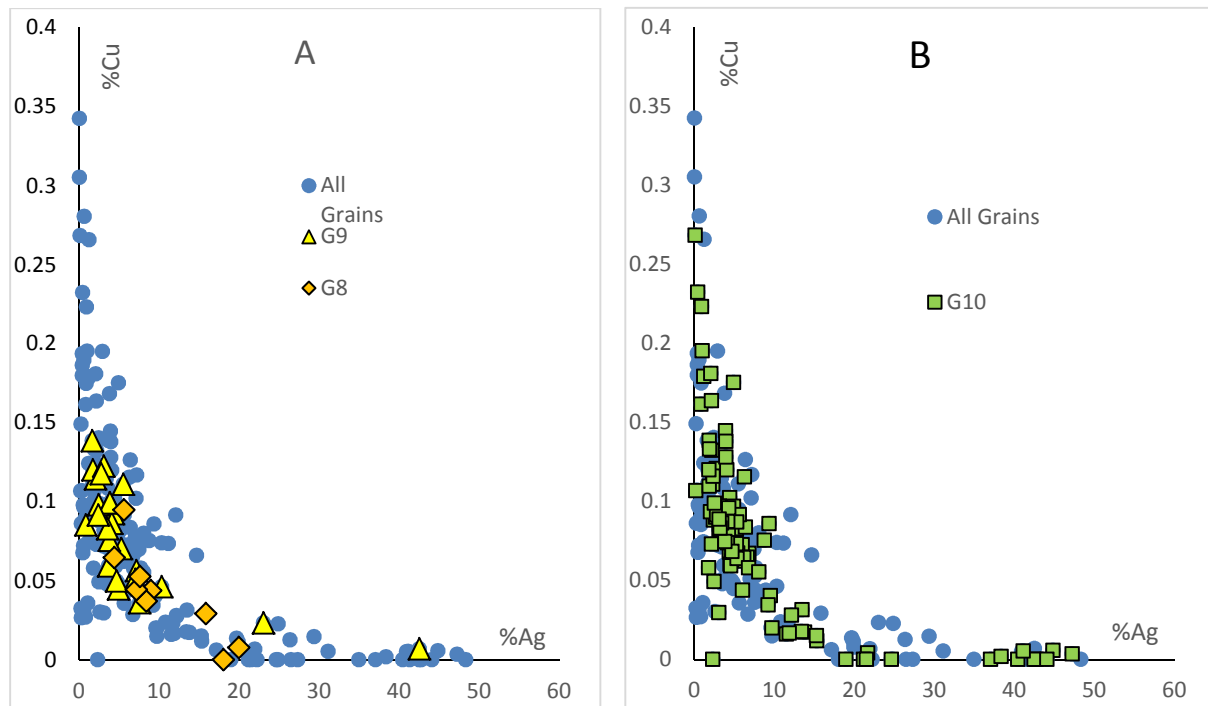
SAMPLE	Inclusion assemblage (Opaque)	Nonopaque	Au Wt%	Ag Wt%	Cu Wt%	TOTAL
G1	Fe oxide		88.70	11.10	0.04	99.98
G3		Ca- amphibole	98.04	1.73	0.11	99.99
G3	Ilmenite		96.10	3.56	0.05	99.94
G4	Fe oxide		96.62	2.87	0.05	99.75
G4	Fe oxide		89.64	10.20	0.07	100.00
G6		Tremolite	97.30	2.34	0.10	99.99
G7		Calcium carbonate	95.70	4.08	0.07	99.99
G8	Fe oxide +Cr		90.79	8.89	0.05	99.99
G8		Ca,Mg,Fe carbonate	93.12	6.62	0.05	100.00
G9		Olivine. Clinopyroxene	97.80	1.64	0.14	99.80
G9	Fe oxide + Cr. Fe oxide		95.07	3.80	0.08	99.11
G9	Fe oxide + Cr. Fe oxide		96.93	2.45	0.10	99.60
G9	Fe oxide + Cr + V, ilmenite		92.10	7.56	0.04	99.89
G9		K spar	56.79	42.53	0.01	99.40
G9		FeMg carbonate	94.95	4.68	0.05	99.86
G10	Fe oxide, silica		97.46	2.24	0.13	99.97
G10	Fe oxide		94.07	5.57	0.06	99.84
G10	Fe oxide		77.78	21.68	0.00	99.63
G10		Clinopyroxene	86.47	13.40	0.02	100.00
G10	Fe oxide + Cr		96.22	3.16	0.10	99.72
G10	Fe oxide + Cr		78.18	21.55	0.00	99.91
G10	Fe oxide		99.32	0.22	0.11	99.89
G10	Chalcopyrite/Silver sulphide (trace Cu)		90.65	8.79	0.08	99.75
G10	Fe oxide		88.00	11.55	0.02	99.82
G10		Ca carbonate	97.08	2.66	0.09	100.00
G10	Fe oxide + Cr+V		93.59	5.31	0.07	99.21
G10	Fe oxide + Cr		87.71	11.90	0.02	99.79
G10	Pyrrhotite		96.42	2.80	0.09	99.48
G10		Biotite	96.65	3.14	0.08	100.00
G10	Ilmenite		97.60	2.10	0.16	100.00

334

335 4.2.3 Copper (Cu)

336 Majority of the gold grains contain Cu, which can be used with Au alloy in conjunction with
 337 the associated Ag to identify discrete compositional fields (Chapman *et al.* 2017b). Fig. 9
 338 shows the general inverse relationship between Ag and Cu for the whole population of gold
 339 grains. This feature appears to be generic (Moles *et al.* 2013, Chapman *et al.*, 2017b) and it
 340 appears that the Cu content is largely controlled by the Ag content of the Au alloy. Thus, in
 341 the majority of cases, Cu in Au-Ag alloy may not be a useful discriminator. Nevertheless,
 342 figure 9 suggests that there are three main compositional fields, namely high >0.15 wt % Cu,
 343 low Ag, low 0-0.15 wt % Cu and low 0-10 wt% Ag, and low Cu < 0.2 wt % and high Ag >10
 344 wt %.

345



346

347 Fig. 9: Eluvial environments conform to the high Cu field, but a small number do occur
 348 within the high Ag field. A similar approach to the gold grains from the adjacent placer
 349 sample (G10) has been undertaken in Figure 9B, but here the full range of compositions is
 350 represented.

351

352

353 4.2.4. The inclusion assemblage

354 Inclusions were generally between 10 and 20 μm in cross-section to a maximum of 50 μm .
 355 These inclusions occur either as simple minerals or comprise complex intimate associations of
 356 several phases that are described in Table 2. The number of inclusions recorded in the 221
 357 grains was very low, however, it is clear that iron oxide \pm Cr and V is the most important
 358 single inclusion specie. Chalcopyrite, pyrrhotite, and acanthite were also observed. Mineral
 359 inclusion characteristics observed are presented in Figs. 10 and 11.

360

361

362

363

364

365

366

367

368

369

370

371

372

373

374

375

376

377

378

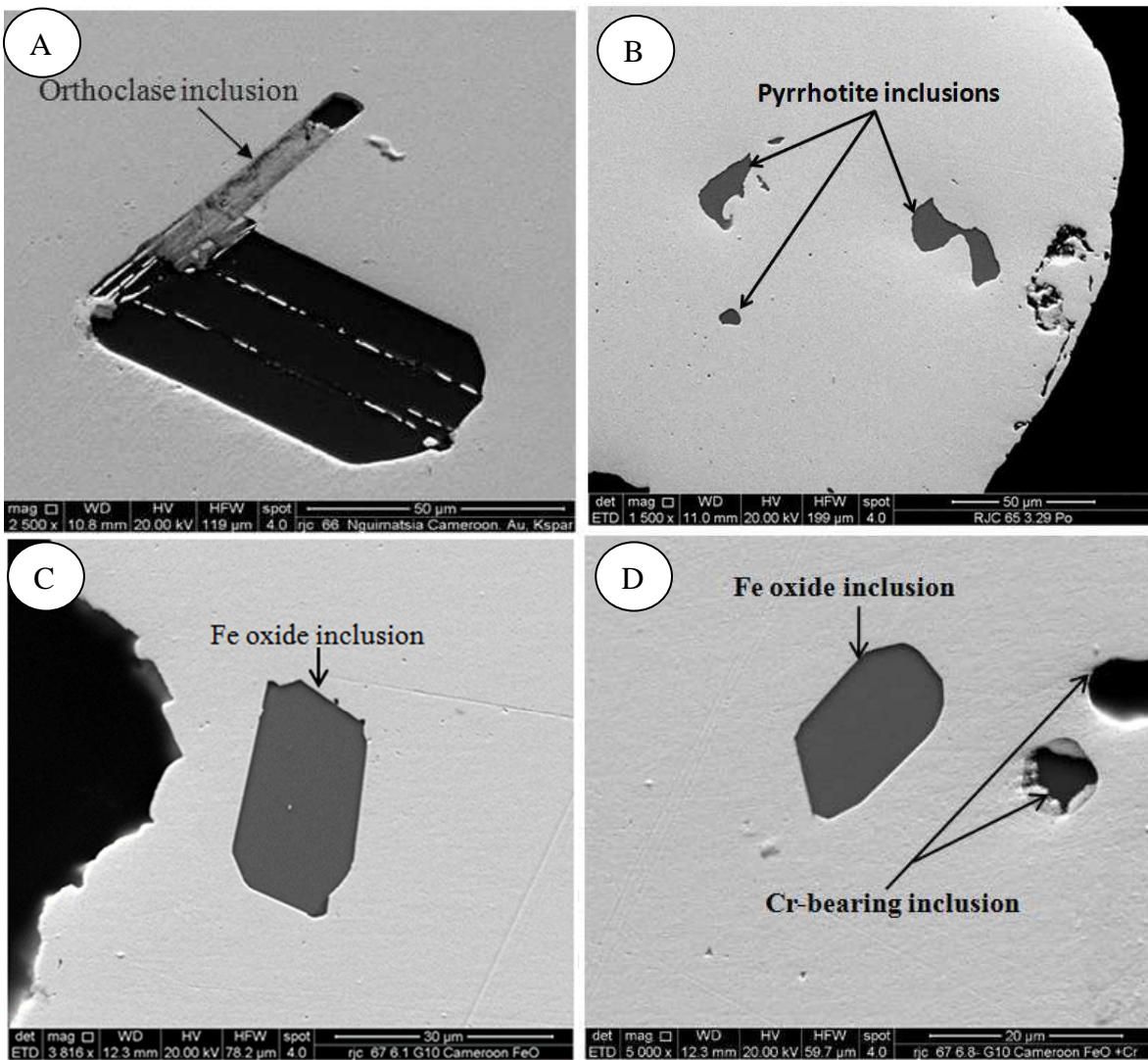
379

380

381

382

383



384

385

386 Fig.10: Back-Scattered Electron (BSE) images of typical inclusions in placer gold grains. (A)

387 Orthoclase inclusion in-filled by Au alloy in gold grain. (B) Pyrrhotite in detrital grain.(C)

388 Typical Fe oxide inclusion in eluvial gold grain. (D) Representative Fe oxide containing about

389 5% of chromium (Cr)

390

391

392

393

394

395

396

397

398

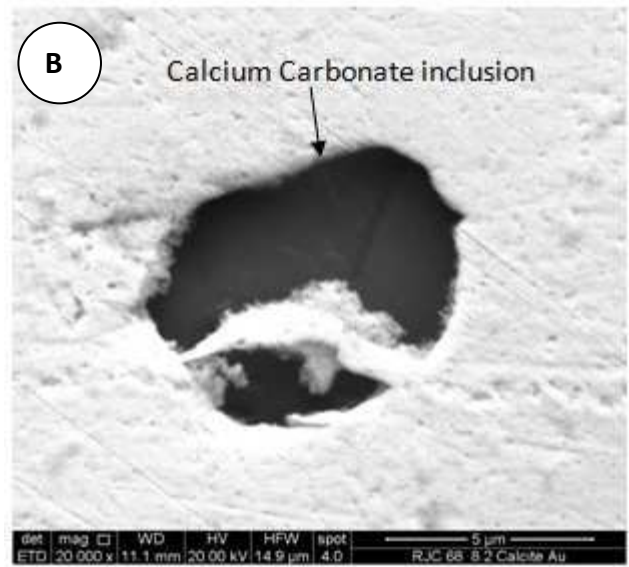
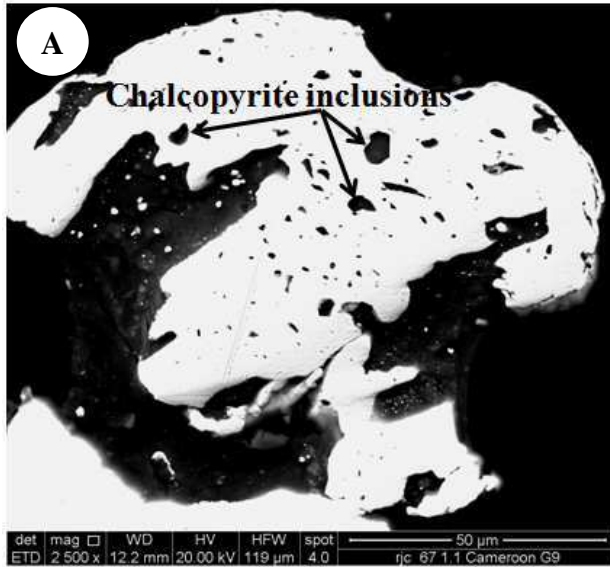
399

400

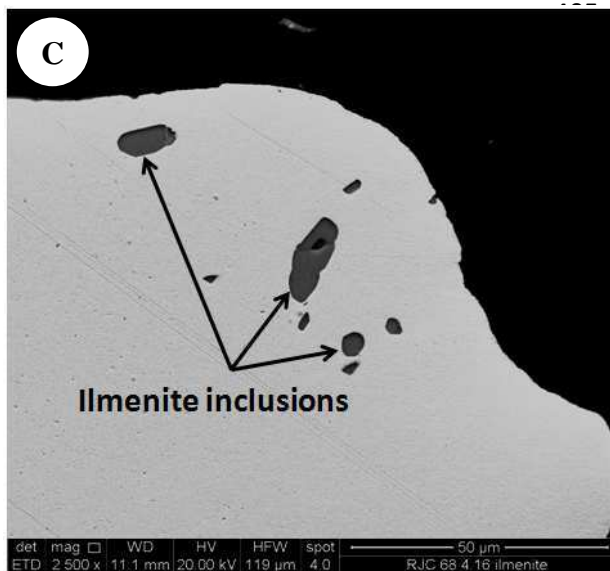
401

402

403



404



414

415

416 Fig.11: Back-scattered Electron (BSE) images of some silicate, carbonate and oxide
 417 inclusions of placer gold grains. (A) Chalcopyrite inclusions in gold grain. (B) Calcium
 418 carbonate inclusion in gold grain from site G7. The calcium carbonate grain is bridged by
 419 secondary Au which postdates it. (C) Ilmenite inclusions in gold grain from site G4.

420

421

422

423

424

425

426 **5. Discussion**

427

428 **5.1. Interpretation of Gold morphology**

429 Eluvial gold from Nkolmedoum (G8 and G9) exhibits a fragile crystalline form and pristine
430 faces bearing the imprint of quartz crystals and/or magnetite, which together provides
431 evidence of very limited transport and therefore a restricted local source. The in-situ source
432 of these gold particles remains unknown; however, a secondary origin may be discounted
433 because of the inclusion suite, which contains chalcopyrite, pyrrhotite, and acanthite.

434

435 **5.2 Interpretation of the Gold Microchemical Signature**

436 Figures 8 and 9 show that there is no single signature which defines all the individual
437 samples. As the gold composition is a proxy for the conditions of precipitation within a
438 hydrothermal regime (Gammons and Williams-Jones 1995), it is concluded that there are
439 different sources of gold in the study area. In this scenario, the eluvial samples are more likely
440 to represent individual gold occurrences and hence show a tighter compositional range. This
441 is consistent with the variation in both Ag and Cu depicted in Figures 8D and 9B.

442

443 The spatial relationships between samples show relationships consistent with their localities.
444 The placer sample from Nkolmedoum (G10) shows characteristics compatible with both local
445 eluvial samples (G8 and G9). The adjacent placer samples of G3 and G4 show the same two
446 ranges of Ag contents, but in different proportions, suggesting differing contributions from
447 the same two source signatures. Similarly, samples G5, G6, and G7 show a consistent Ag
448 range notwithstanding the small sample sizes. Sample G1 is geographically distinct but even
449 so may share the low Ag signature with some grains from the nearest locality of G2. Overall
450 the evidence from alloy signatures suggests that there are multiple sources, which individually
451 may exhibit a restricted Ag range in the regional sample set.

452

453 From the perspective of exploration, it would be highly beneficial to develop an overarching
454 deposit model, and commonly the inclusion assemblages provide the best source of
455 information in this regard. In the majority of studies such as this, the inclusion suite of 'ore
456 minerals' such as sulfides, sulfarsenides and tellurides provide discriminants whereby a
457 signature may be established. In the present study, insufficient sulfide inclusions were
458 observed to apply this approach, and characterization has relied mainly on interpreting the
459 significance of oxide, carbonates and silicate inclusion species. Figure 12 shows the Ag

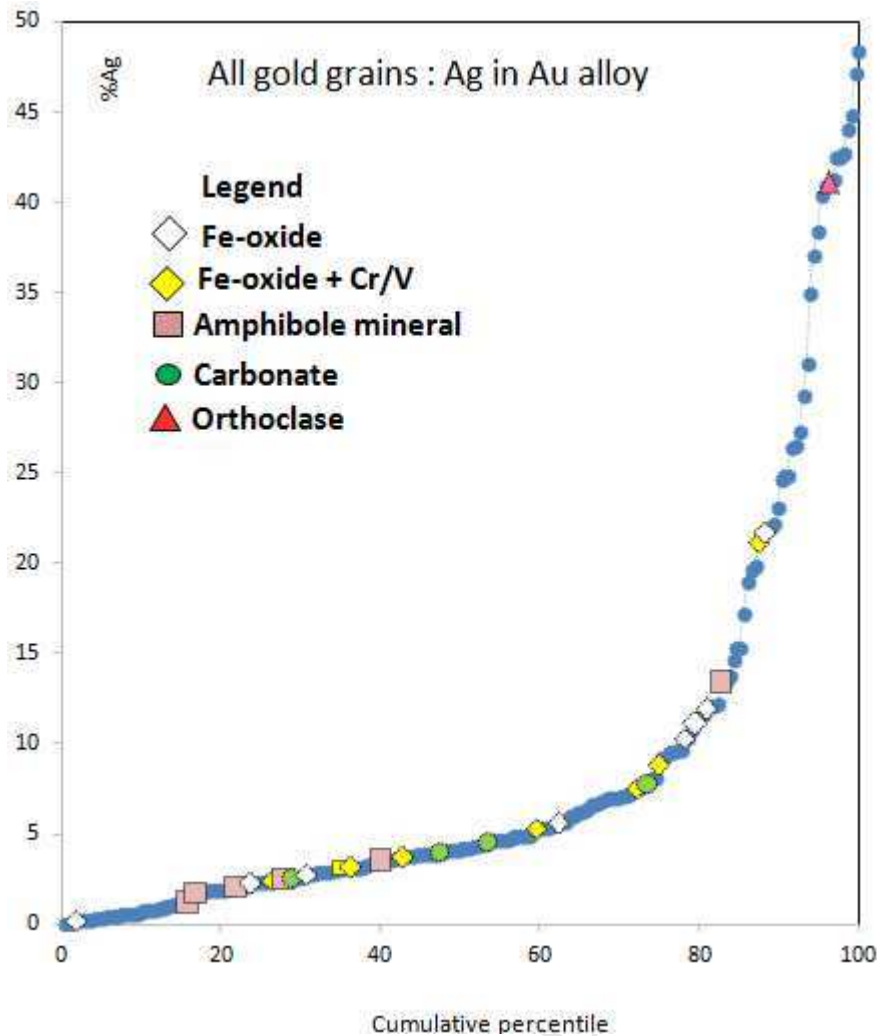
460 compositions of gold grains which host different types of silicate, oxide and carbonate
461 inclusions. Low inclusion abundance precludes the identification of clear compositional
462 fields, but there is no clear correlation between inclusion species and Ag content, except that
463 inclusions may be scarce in higher Ag gold alloy.

464
465 Magnetite inclusion within gold showed a range of Cr and V in the 0-c 5% range, as measured
466 by semi quantitative analysis by EDS. These concentrations are far higher than those recorded
467 in hydrothermal magnetite from several ore deposit types (Nadoll et al. 2014). These authors
468 report the highest values of a few thousand ppm in magnetite from magmatic hydrothermal
469 systems, but these values are up to an order of magnitude lower than those recorded in the
470 present study. Nadoll et al. (2014) note that incorporation of V in the magnetite lattice
471 increases with both temperature and decreasing fO_2 , and a reducing environment is consistent
472 with the observation of a pyrrhotite inclusion in another gold grain. These authors also note
473 that some of the highest Cr and V values in magnetite in magmatic hydrothermal systems
474 were a consequence of fluid- wall rock interaction.

475
476 The presence of amphibole minerals within the gold grains is challenging to interpret in the
477 absence of the petrology of the hypogene ore. The presence of these minerals suggests a
478 relationship with amphibolites, but the mechanism of their incorporation into particulate gold
479 remains unclear.

480 The presence of calcite and ankeritic dolomite inclusions is compatible with interaction of a
481 CO_2 – rich fluid with mafic lithologies. Additionally the presence of a quartz inclusion
482 indicates a mineralizing fluid not in equilibrium with an amphibolite. In summary,
483 substantially evidence of the gold mineralization suggests mineralizing fluids in equilibrium
484 with amphibolite (likely reducing) and that this interaction accounts for the mineralogy and
485 geochemistry of the inclusion suite within the gold. Some of the gold appears to have been
486 deposited by mineralizing fluids in equilibrium with felsic rocks (hence the quartz and K-
487 feldspar inclusions) and oxidizing (hence carbonate inclusions). It also seems likely that the
488 fluids were relatively hot and reducing, promoting high Cr and V substitution in magnetite.

489
490
491



493

494 Figure 12: Relationship between inclusion species and host alloy.

495

496

497 **5.3 Comparison of gold signature with those associated with other styles of** 498 **mineralization**

499

500 The gold signature recorded in this study is distinct from those reported for other styles of
 501 mineralization globally. The available evidence suggests that hot reducing fluids interacted
 502 with amphibolites to generate the inclusion signature observed here. This mechanism would
 503 explain major differences between the signatures of the gold studied here and those recorded
 504 in gold from other mineralizing systems globally. An overview of gold microchemical
 505 signatures from different deposit styles was provided by Chapman et al. (2009). Gold from
 506 Phanerozoic orogenic settings typically exhibits an inclusion signature of sulfides \pm
 507 sulfarsenides \pm sulfosalts, whereas gold from Archaean orogenic mineralization often yielded a

508 Bi-Te association. Subsequent detailed studies of gold from other Phanerozoic orogenic gold
509 areas in the Canadian Cordillera have reinforced this compositional template, (Chapman et al
510 2010a,b, 2016). Gold from magmatic hydrothermal system has proved to be compositionally
511 distinct, as calc alkaline porphyries and associated epithermal systems in Yukon showed a
512 generic Bi-Pb-Te-S association in the inclusion assemblage (Chapman et al 2017b) whereas
513 gold from alkalic porphyry systems in British Columbia were identifiable through their Hg-Pd
514 inclusion signature (Chapman et al. 2017a).

515
516 Finally, various studies have suggested a mechanism of gold growth in tropical environments,
517 (e.g. *Bowell et al. 1993*) however the nature of the mineral inclusions recorded in this study
518 demonstrate that the gold grains are detrital in origin and preserve hypogene mineralogy as
519 inclusions.

520

521 **6. Conclusions**

522

523 Studies of eluvial and placer gold grains from the Meyos-Essabikoula area within the
524 Precambrian basement complex of Southern Cameroon have constrained the nature of the
525 hypogene sources, which remain undiscovered. Morphologically, placer gold grains show a
526 wide variety of shapes, but the fragile crystalline form and pristine faces on most eluvial
527 grains provides evidence of very limited transport and therefore a restricted local source.
528 Subtle differences in the Ag contents of populations of gold grains supports a hypothesis of
529 multiple sources, which are represented to varying degrees in the placer populations
530 according to their spatial relationship with different drainages. Although the in-situ sources of
531 these gold particles remains unknown, a secondary origin may be discounted because of the
532 mineralogy of the inclusion suite.

533 Overall the gold alloy composition is predominantly a binary Au-Ag alloy with minor
534 contribution from Cu.

535

536 The alloy composition alone is not particularly diagnostic of a specific source style or host
537 lithology, however Fe-oxide inclusions, sometimes containing Cr and V, are relatively
538 common and suggest that the ore fluids interacted with local amphibolite, a hypothesis
539 consistent with the presence of carbonate inclusions. Interpretation of the V and Cr content of
540 magnetite suggest that these fluids were reducing and relatively hot.

541 This study has provided a platform for further exploration to investigate the significance of
542 the gold- amphibolite association suggested here. The project outcomes provide a clear
543 example of the benefit of gold grain studies in terranes of poor exposure.

544

545 **Acknowledgments**

546 This article is part of the PhD thesis of Nguimatsia-Dongmo Franck Wilfried at Pan African
547 University Life and Earth Science institute; supervised by A.T. Bolarinwa (University of
548 Ibadan, Nigeria) and R.F. Yongue (University of Yaounde 1, Cameroon); supported through
549 the African Union Scholarship scheme, to which we are grateful. We are indebted to Dr
550 Ndong Bidzang Francois, Christopher Fuanya and Djou Ernest for their help during the field
551 work and sample collection. We are extremely grateful for the efforts of the reviewers and for
552 the comments of the Editor Damien Delvaux, which have all greatly enhanced the quality of
553 the manuscript.

554

555

556 **REFERENCES**

557

558 Bessoles, B. and Trompette, M.,1980. Geologie de l'Afrique: La chaine panafricaine, "zone
559 mobile d'Afrique Central (partie sud) et zone mobile soudanaise". Memoire du Bureau de
560 Recherche Geologiques et Minieres, 92, 396.

561

562 Bowell, R.J., Foster, R.P. and Gize, A.P., 1993. The mobility of gold in tropical rain forest
563 soils. *Economic Geology*, 88(5), pp.999-1016.

564

565 Chapman, R.J., Leake, R.C., Moles, N.R. et al., 2000a. The application of microchemical
566 analysis of gold grains to the understanding of complex local and regional gold
567 mineralization: A case study in Ireland and Scotland. *Economic Geology*, 95, 1753–1773.

568

569 Chapman, R.J., Leake, R.C. & Moles, N.R., 2000b. The use of microchemical analysis of
570 alluvial gold grains in mineral exploration: Experiences in Britain and Ireland. *Journal of
571 Geochemical Exploration*, 71, 241–268. [https://doi.org/10.1016/S0375-6742\(00\)00157-6](https://doi.org/10.1016/S0375-6742(00)00157-6)

572

573 Chapman, R. J., Leake, R. C., Bond, D. P. G., Stedra, V., and Fairgrieve, B. 2009. Chemical
574 and mineralogical signatures of gold formed in oxidizing chloride hydrothermal systems and
575 their significance within populations of placer gold grains collected during reconnaissance.
576 *Economic Geology*, 104(4), 563-585. <https://doi.org/10.2113/gsecongeo.104.4.563>

577

578 Chapman R.J, Mortensen J.K. 2016. Characterization of gold mineralization in the northern
579 Cariboo gold district, British Columbia, Canada, through integration of compositional studies
580 of lode and detrital gold with historical placer production: A template for evaluation of
581 orogenic gold districts. *Economic Geology*. **111**(6), pp. 1321-1345

582

- 583 Chapman R.J., Mileham T.J., Allan M.M, Mortensen J.K., 2017a. A distinctive Pd-Hg
584 signature in detrital gold derived from alkalic Cu-Au porphyry systems. *Ore Geol Rev* 83:84–
585 102. <https://doi.org/10.1016/j.oregeorev.2016.12.015>.
586
- 587 Chapman R.J., Allan M.M., Mortensen J.K., Wrighton T.M., Grimshaw M.R., 2017b. A new
588 indicator mineral methodology based on a generic Bi-Pb-Te-S mineral inclusion signature in
589 detrital gold from porphyry and low/intermediate sulfidation epithermal environments in
590 Yukon Territory, Canada. *Mineralium Deposita*. <https://doi.org/10.1007/s00126-017-0782-0>
591
- 592 Clifford, T. N., Kennedy, W. Q., Gass, I. G., 1970. African magmatism and tectonics: a
593 volume in honour of W Q Kennedy. Hafner Pub. Co.
594
- 595 Crawford, E.C., 2007. New tools for examining morphology, composition and crystallinity:
596 Unpublished M.Sc. thesis, The University of British Columbia, Vancouver; p. 1-167
597
- 598 Foster, R. P., & Piper, D. P., 1993. Archaean lode gold deposits in Africa: crustal setting,
599 metallogenesis and cratonization. *Ore Geology Reviews*, 8(3-4), 303-347.
600 [https://doi.org/10.1016/0169-1368\(93\)90021-P](https://doi.org/10.1016/0169-1368(93)90021-P)
601
- 602 Gammons, C.H. & Williams-Jones, A.E., 1995. Hydrothermal geochemistry of electrum:
603 Thermodynamic constraints. *Economic Geology*, 90, 420–432.
604 <https://doi.org/10.2113/gsecongeo.90.2.420>
605
- 606 Goodwin A. M., 1991. Precambrian Geology. *The Dynamic Evolution of the Continental*
607 *Crust*.
608
- 609 Hancock, E.A. & Thorne, E.M., 2011. Mineralogy of lode and alluvial gold from the Western
610 Capricorn Orogen, Western Australia. *Australian Journal of Earth Sciences*, 58, 793–801.
611 <https://doi.org/10.1080/08120099.2011.605802>
612
- 613 Knight, J. B., Mortensen, J. K., and Morison, S. R. 1999a. Lode and placer gold composition
614 in the Klondike District, Yukon Territory, Canada; implications for the nature and genesis of
615 Klondike placer and lode gold deposits. *Economic Geology*, 94(5), 649-664.
616 <https://doi.org/10.2113/gsecongeo.94.5.649>
617
- 618 Knight, J. B., Morison, S. R., and Mortensen, J. K. 1999b. The relationship between placer
619 gold particle shape, rimming, and distance of fluvial transport as exemplified by gold from the
620 Klondike District, Yukon Territory, Canada. *Economic Geology*, 94(5), 635-648.
621 <https://doi.org/10.2113/gsecongeo.94.5.635>
622
- 623 Kornprobst, J., Lasserre, M., Rollet, M., Soba, D., 1976. Existence au Cameroun d'un
624 magmatisme alcalin Pan-Africain ou plus ancien: la syénite néphélinique de Nkonglong.
625 Comparaison avec les roches alcalines connues dans la même région. *Bulletin Société*
626 *Géologique de France* 18 (5), 1295–1305 tome XVIII.
627
- 628 Lasserre, M., Soba, D., 1976. Age Libérien des granodiorites et des gneiss à pyroxènes du
629 Cameroun Méridional. *Bulletin BRGM* 2 (4), 17–32.
630

- 631 Leake R, Chapman R, Bland D, Condliffe E, Styles M., 1997. Microchemical characterization
632 of gold from Scotland. *Trans Inst Min Metal* 106 B *Appl Earth Sci* 102:65–82.
633
- 634 Li, X. H., Chen, Y., Li, J., Yang, C., Ling, X. X., and Tchouankoue, J. P. (2016). New isotopic
635 constraints on age and origin of Mesoarchean charnockite, trondhjemite and amphibolite in
636 the Ntem Complex of NW Congo Craton, southern Cameroon. *Precambrian Research*, 276,
637 14-23. <http://dx.doi.org/10.1016/j.precamres.2016.01.027>
638
- 639 Maurizot, P., Abessolo, A., Feybesse, J. L., Johan, V., and Lecomte, P. 1986. Etude et
640 prospection minière du Sud-Ouest Cameroun. Synthèse des travaux de 1978 à 1985. *Rapport*
641 *bureau de recherches géologiques et minières* 85 Cameroun, 66, 274p.
642
- 643 McLenaghan, M. B., and Cabri, L. J. 2011. Review of gold and platinum group element
644 (PGE) indicator minerals methods for surficial sediment sampling. *Geochemistry Exploration*
645 *Environment Analysis* 11 (4):251-263 · DOI: 10.1144/1467-7873/10-IM-026
646
- 647 Moles, N.R., Chapman RJ, Warner R., 2013. The significance of copper concentrations in
648 natural gold alloy for reconnaissance exploration and understanding gold-depositing
649 hydrothermal systems. *Geochem Expl Env Anal* 13(2):115–130. [https://doi.org/10.1144/](https://doi.org/10.1144/geochem2011-114)
650 [geochem2011-114](https://doi.org/10.1144/geochem2011-114).
651
- 652 Naden, J., Styles, M.T., and Henney, P.J., 1994. Characterization of gold from Zimbabwe:
653 Part 1, bedrock gold: British Geological Survey, Technical Report WC/94/51, 18 p.
654 Nadoll, P., Angerer, T., Mauk, J.L., French, D. and Walshe, J., 2014. The chemistry of
655 hydrothermal magnetite: A review. *Ore Geology Reviews*, 61, pp.1-32.
656
- 657 Nadoll, P., Angerer, T., Mauk, J. L., French, D., and Walshe, J. 2014. The chemistry of
658 hydrothermal magnetite: A review. *Ore Geology Reviews*, 61, 1-32.
659
- 660 Nédelec, A. Nsifa, E. N. Martin, H., 1990. Major and trace element geochemistry of the
661 Archean Ntem plutonic complex (South Cameroon): petrogenesis and cristal evolution, *Prec.*
662 *Ress.*, 35-50pp.
663
- 664 Nsifa E. N. and Riou R., 1990. Post-Archaean migmatization in the charnockitic series of the
665 Ntem Complex, Congo Craton, southern Cameroon. In 15th Colloquium on African Geology,
666 pp. 33-36. Publications Occasionnelle, CIFEG, University of Nancy I.
667
- 668 Omang B.O. , C.E. Suh , B. Lehmann , A. Vishiti , N.N. Chombong , A.N. Fon , J.A. Egbe ,
669 E.M. Shemang., 2015. Microchemical signature of alluvial gold from two contrasting
670 terrains in Cameroon.
671
- 672 Potter, M., Styles, M.T., 2003. Gold characterization as a guide to bedrock sources for the
673 Estero Hondo alluvial gold mine, western Ecuador. *Trans Inst Min Metall B Appl Earth Sci*
674 <https://doi.org/10.1179/037174503225011261>
675
- 676 Rocci, G., 1965. Essai d'interpretation de mesures geochronologiques. La structure de l'Ouest
677 africain. *Sciences Terre Nancy*, 10, 461-479.
678

- 679 Shang, C.K., 2001a. Geology, geochemistry and geochronology of Archaean rocks from the
680 Sangmelima Region, Ntem complex, NW Congo craton, South Cameroon. Ph.D Thesis,
681 University of Tübingen, Germany, pp. 313.
682
- 683 Shang, C.K., Satir, M., Siebel, W., Taubald, H., Nsifa, E.N., Westphal, M., Reitter, E., 2001b.
684 Genesis of K-rich granitoids in the Sangmelima region, Ntem complex (Congo craton),
685 Cameroon. *Terra Nostra* 5, 60–63.
686
- 687 Suh C. E., Lehmann B., and Mafany G. T., 2006. Geology and geochemical aspects of lode
688 gold mineralization at Dimako-Mboscorro, SE Cameroon. *Geochemistry: Exploration,
689 Environment, Analysis* 6(4), 295-309. <https://doi.org/10.1144/1467-7873/06-110>
690
- 691 Tchameni, R., 1997. Géochemie et géochronologie des formations de l'Archéen et de
692 Paléoprotérozoïque du Sud Cameroun (Groupe du Ntem, Craton du Congo). Thèse de
693 Doctorat de l'Université d'Orléans, 395 pp.
694
- 695 Tchameni R., Mezger K., Nsifa N. E., and Pouclet A., 2000. Neoarchaean crustal evolution in
696 the Congo Craton: evidence from K rich granitoids of the Ntem Complex, southern
697 Cameroon. *Journal of African Earth Sciences* 30(1), 133-147. [https://doi.org/10.1016/S0899-
698 5362\(00\)00012-9](https://doi.org/10.1016/S0899-5362(00)00012-9)
699
- 700 Tchameni R., Mezger K., Nsifa N. E., and Pouclet A., 2001. Crustal origin of Early
701 Proterozoic syenites in the Congo Craton (Ntem Complex), South Cameroon. *Lithos* 57(1),
702 23-42. [https://doi.org/10.1016/S0024-4937\(00\)00072-4](https://doi.org/10.1016/S0024-4937(00)00072-4)
703
704
- 705 Tchameni, R., Lerouge, C., Penaye, J., Cocherie, A., Milesi, J. P., Toteu, S. F., and Nsifa, N.
706 E. 2010. Mineralogical constraint for metamorphic conditions in a shear zone affecting the
707 Archean Ngoulemakong tonalite, Congo craton (Southern Cameroon) and retentivity of U–Pb
708 SHRIMP zircon dates. *Journal of African Earth Sciences*, 58(1), 67-80.
709 <https://doi.org/10.1016/j.jafrearsci.2010.01.009>
710
- 711 Toteu, S.M., Van Schmus, W.R., Penaye, J., Nyobe, J.B., 1994. U–Pb and Sm–Nd evidence
712 for Eburnian and Pan-African high grade metamorphism in cratonic rocks of Southern
713 Cameroon. *Precambrian Research* 67, 321–347.
714 [https://doi.org/10.1016/0301-9268\(94\)90014-0](https://doi.org/10.1016/0301-9268(94)90014-0)
715
- 716 Townley, B. K., Herail, G., Maksaev, V., Palacios, C., de Parseval, P., Sepuldeva, F.,
717 Orellana, R., Rivas, P. & Ulloa, C. 2003. Gold grain morphology and composition as an
718 exploration tool: application to gold exploration in covered areas. *Geochemistry: Exploration,
719 Environment, Analysis*, 3, 29–38.
720
- 721 Vicat, J.P., Leger, J.M., Nsifa, E., Piguët, P., Nzenti, J.P., Tchameni, R., Pouclet, A., 1996.
722 Distinction au sein du craton congolais du Sud-Ouest du Cameroun, de deux épisodes
723 doléritiques initiant les cycles orogéniques éburnéen (Paléoprotérozoïque) et Pan- Africain
724 (Néoprotérozoïque). *Compte Rendu de l'Académie des Sciences Paris* 323, 575–582 séries II
725 a.
726

Figures

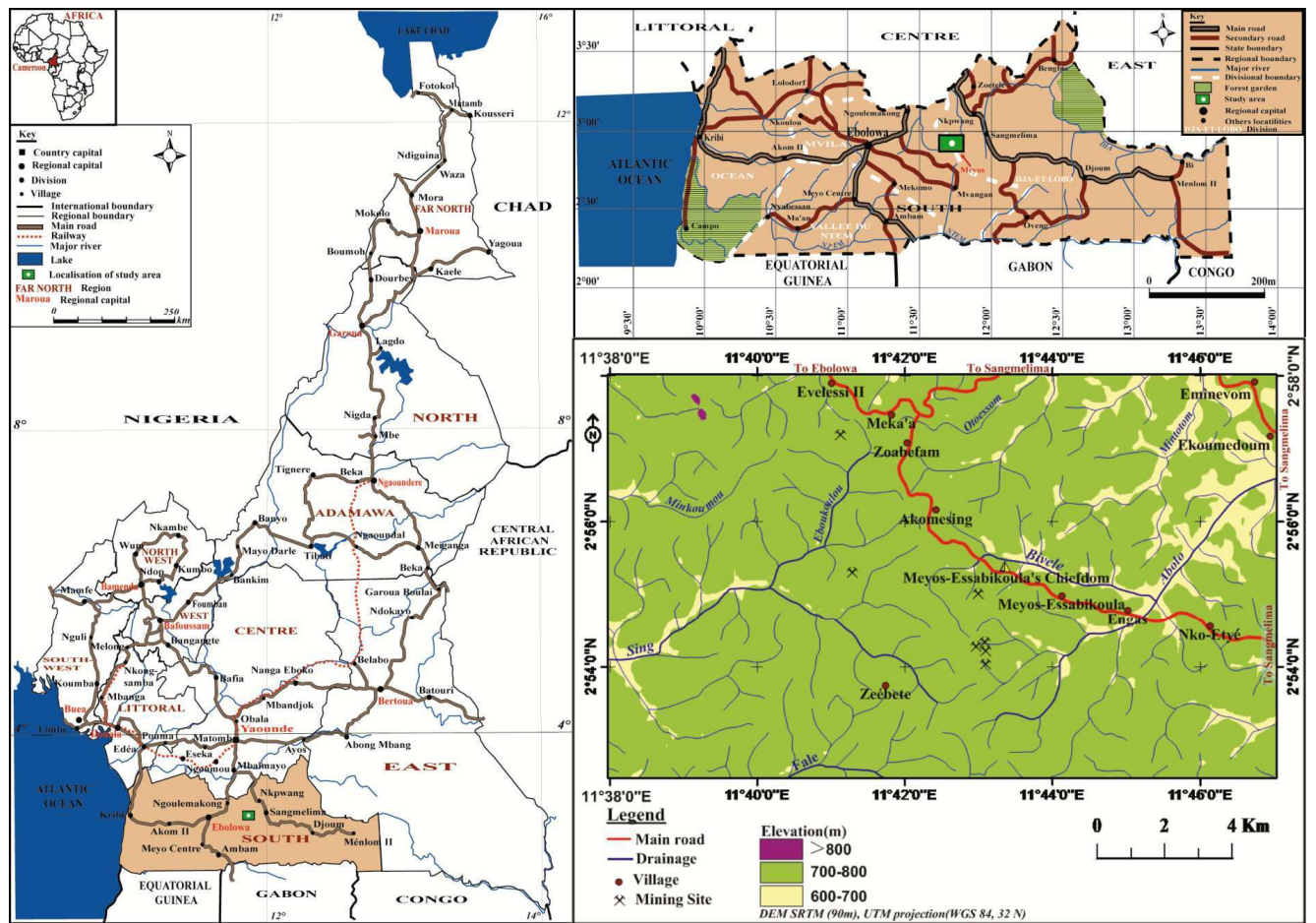
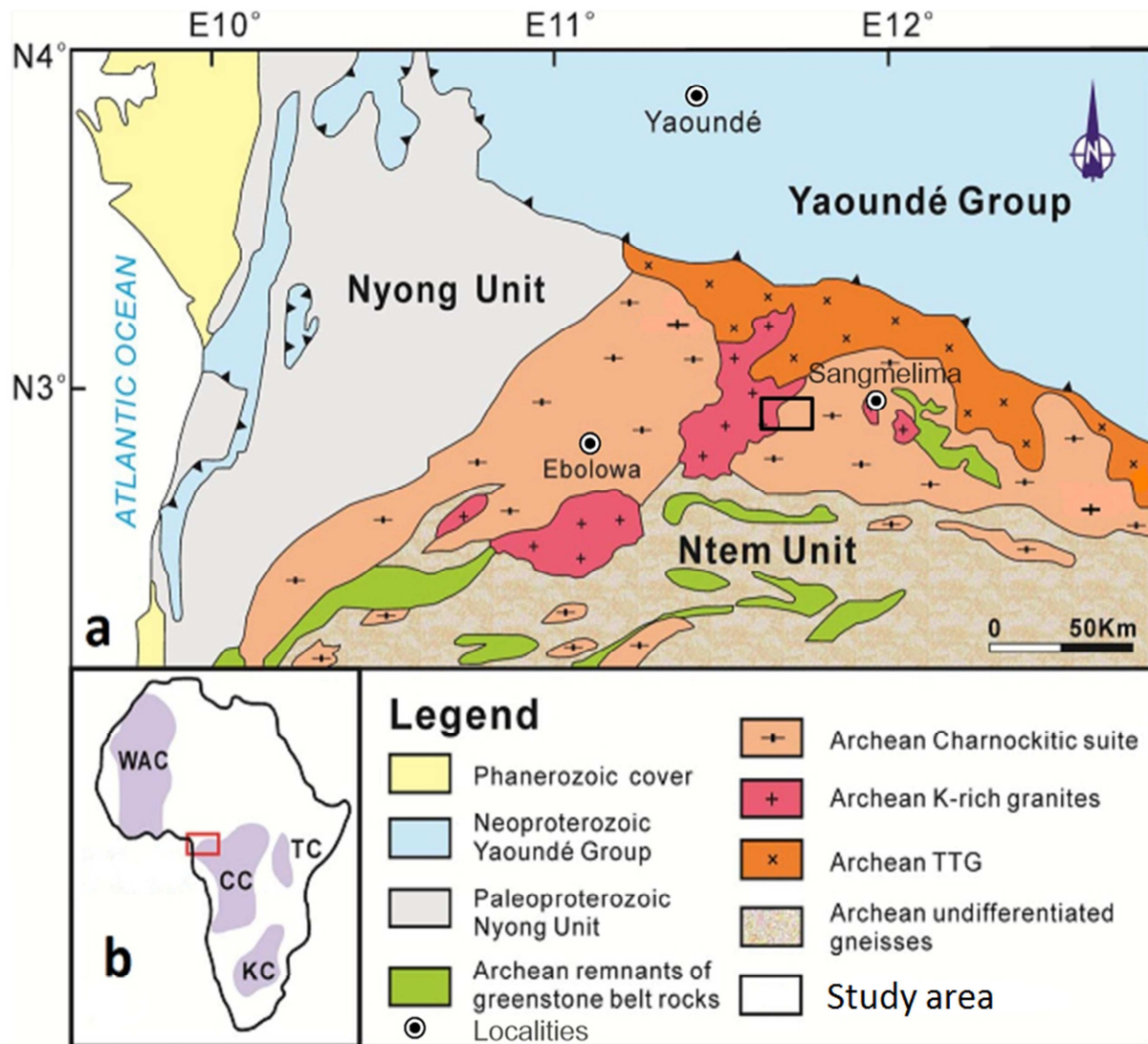


Fig.1: Location map of Meyos Essabikoula showing the road map of Cameroon with an inset of the map of Africa (top left), the road map of the South Region of Cameroon (top right) and the road map of Meyos Essabikoula, showing artisanal mining sites.



(Fig.2): a-Geological sketch map of southwestern Cameroon (modified after Maurizot *et al.*, 1986; Tchameni *et al.*, 2010); b- showing the major Precambrian units and WAC: West African Craton; CC: Congo Craton; TC: Tanzanian Craton; KC: Kapvaal Craton.) (In Li *et al.*, 2016).

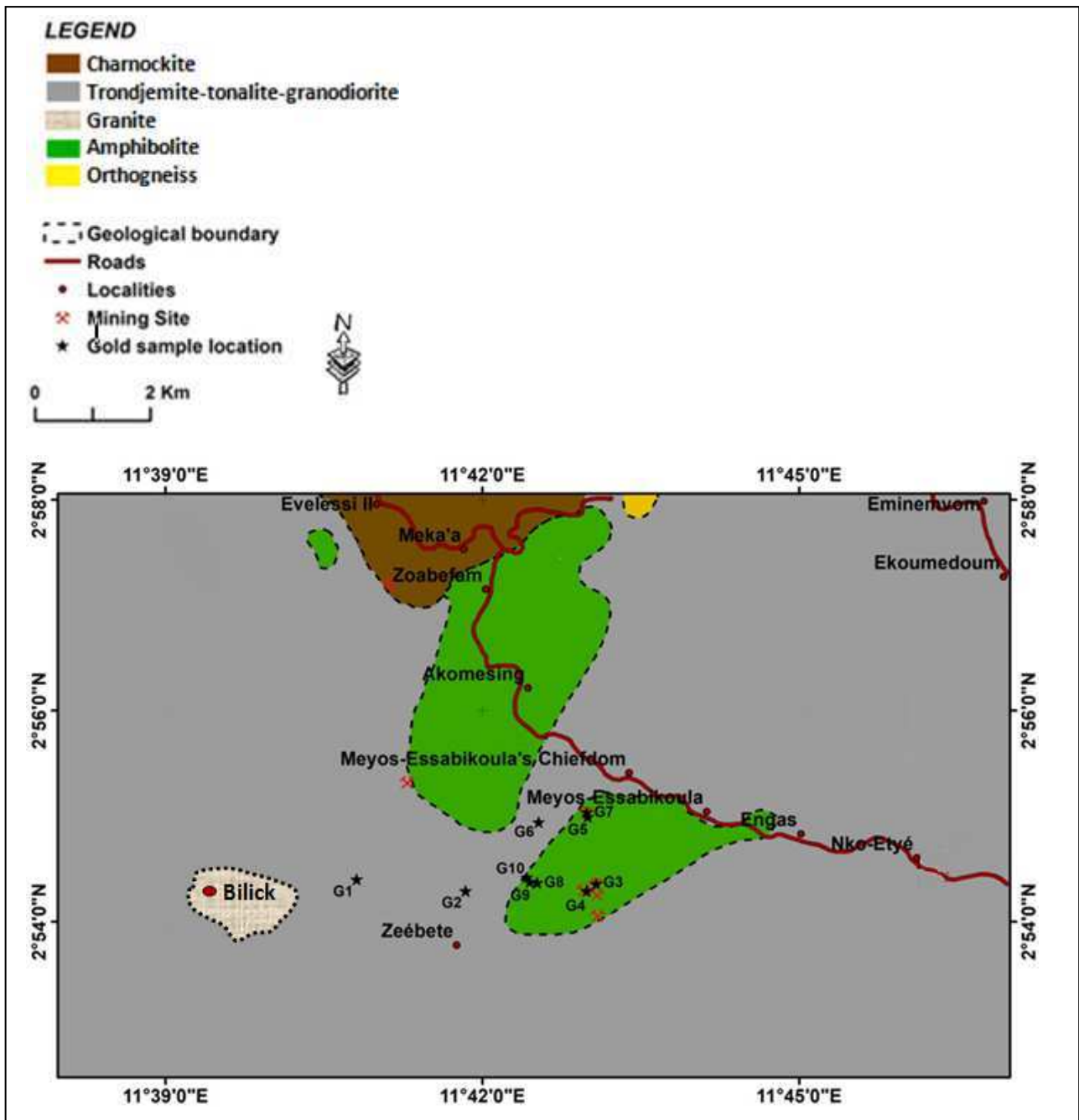


Fig.3: Sketch geological map of study area, showing the distribution of rock out crops and placer gold occurrences.



Fig.4: (A) methodology of collection of gold grains. (B) Example of an excavated pit at Gatan locality.

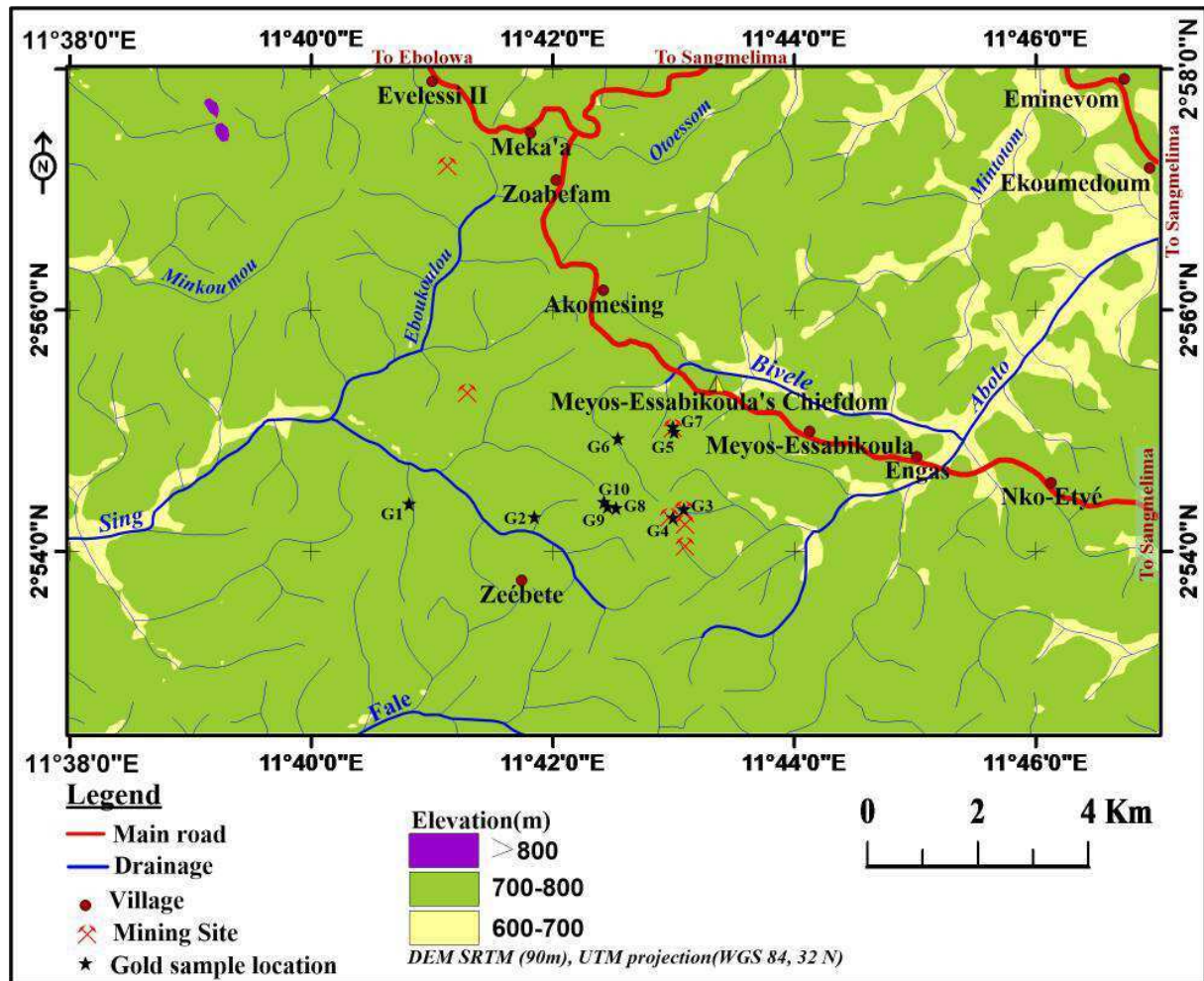


Figure: 5: Sample location in relation to the tributaries of the Sing and Bivele Rivers

G1, G2: Bilick ; G3 : Zalom; G4, G5,G6,G7: Gatan; G8,G9,G10: Nkolmedoum

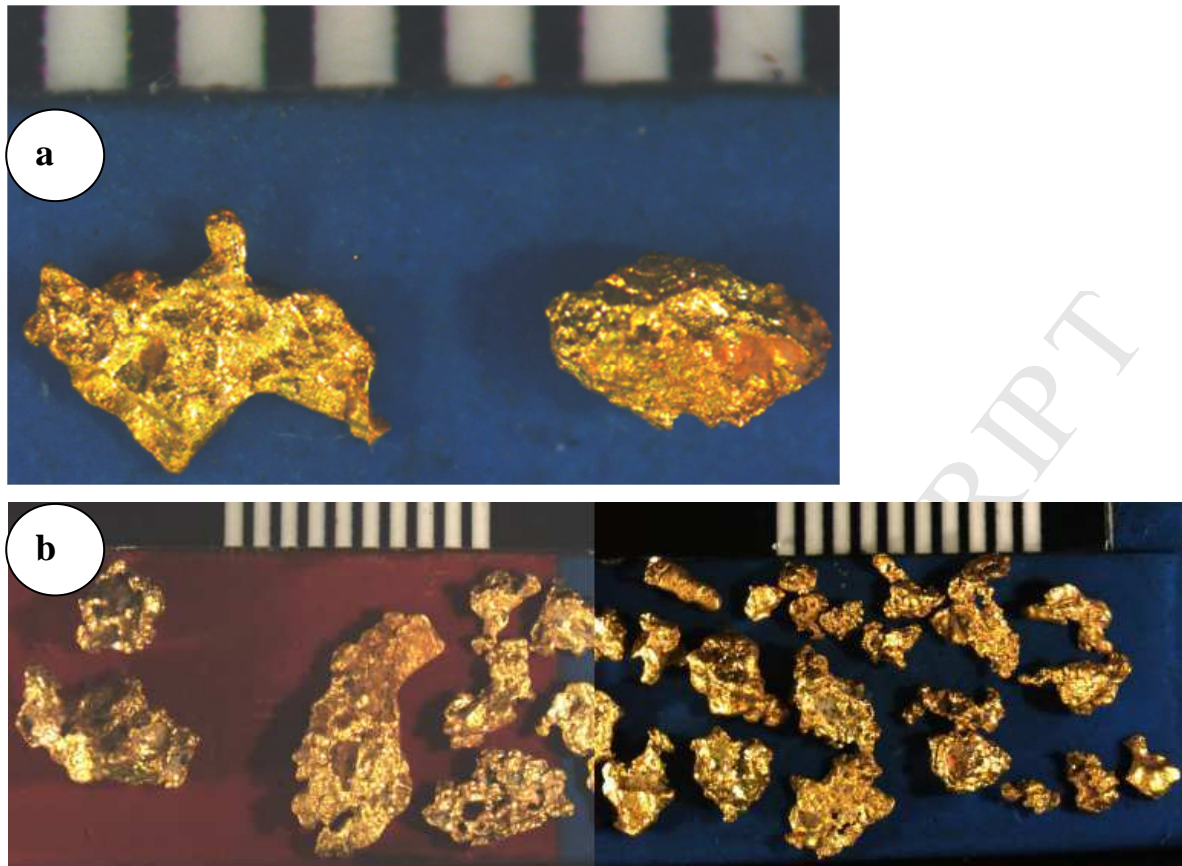


Fig.6a: Angular Gold grains defined as Group 1. Scale bar is in mm. Sample from Nkolmedoum locality.

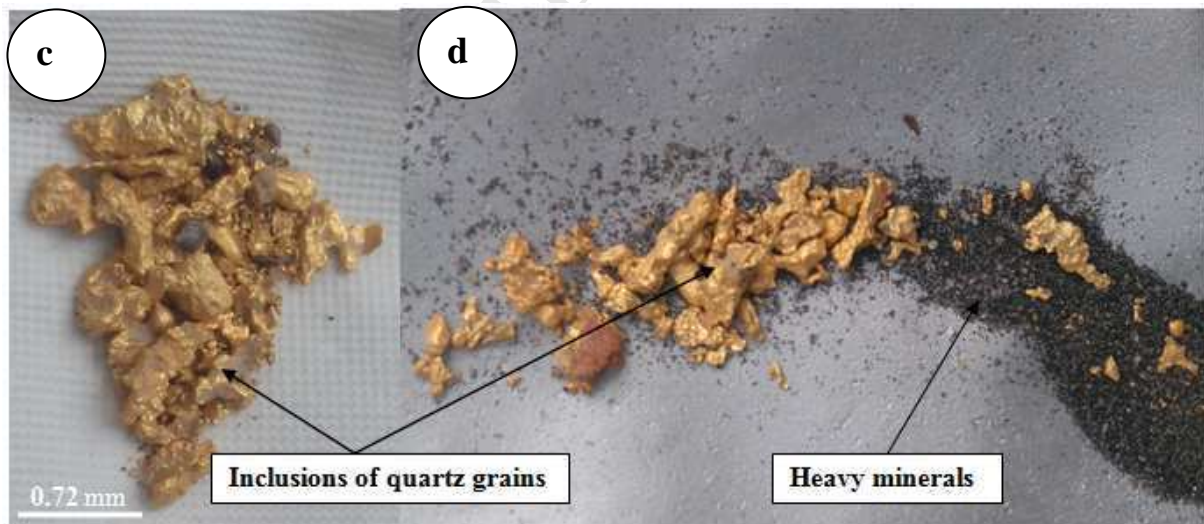


Fig.6 (c and d): Gold grains recovered from G8 and G9 localities captured immediately after panning showing adhering quartz grains and associated heavy minerals.

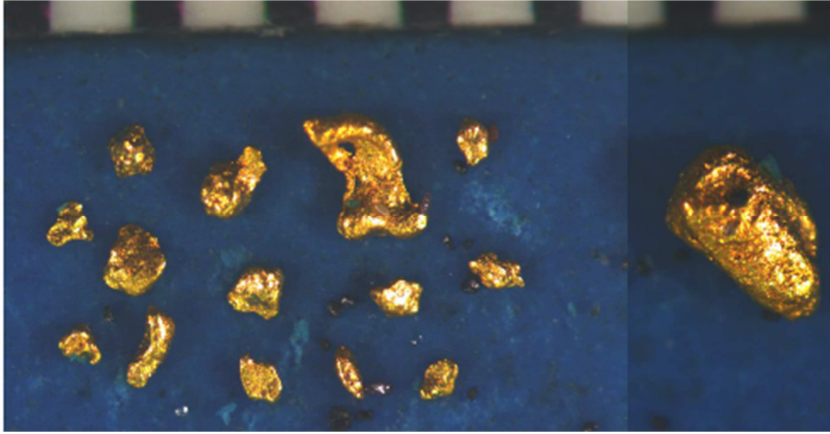


Fig.7: Group 2- rounded to elongate alluvial gold grains from Nkolmedoum. The general outline of these grains is regular and surface topography tends to be smooth (Scale bar in mm).

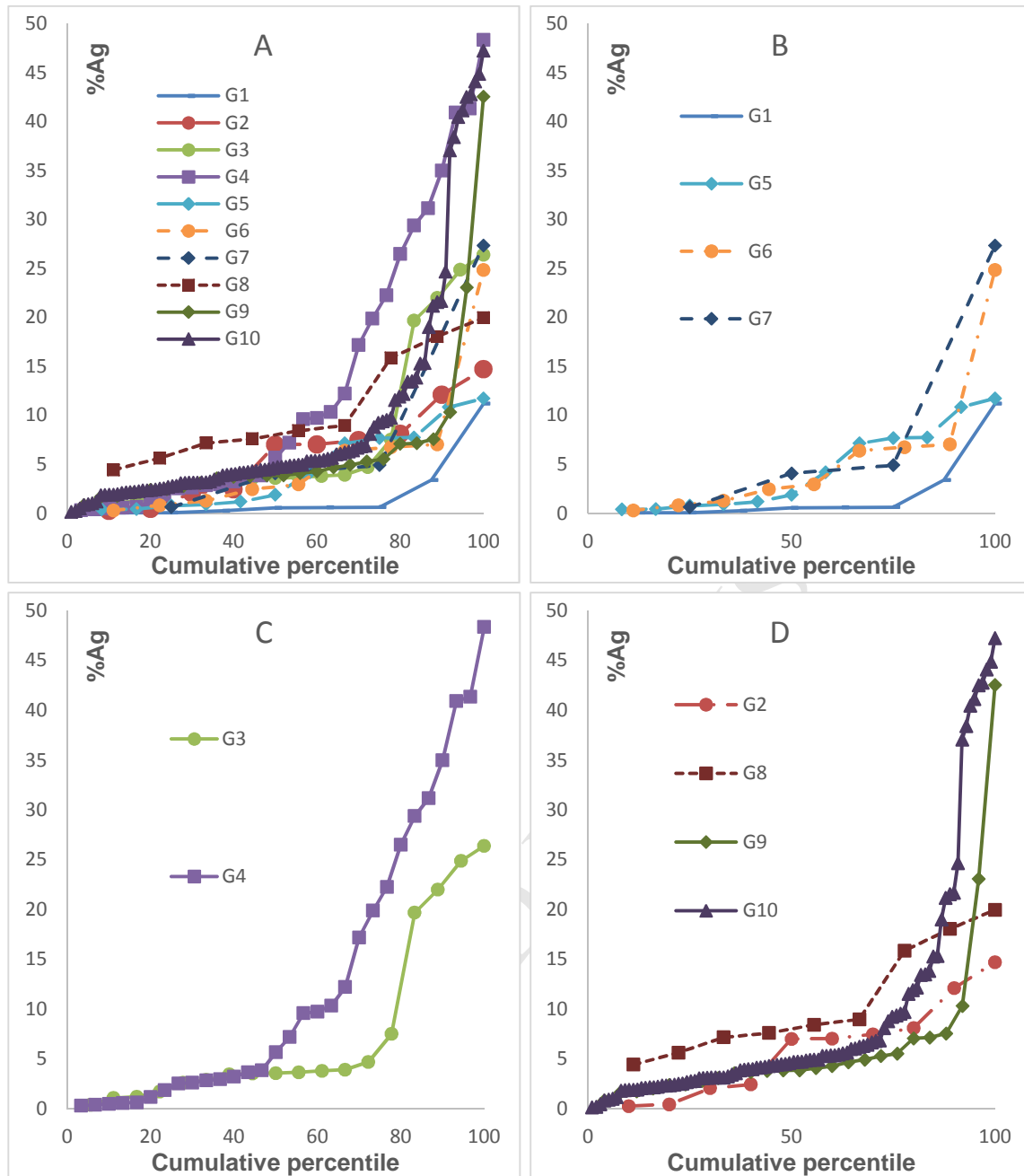


Fig. 8: Silver content of populations of gold grains from the study area: (A) comparison of signatures from all populations studied;(B): Comparison of signatures from adjacent placer localities, plus G1;(C): Comparison of the signatures of gold from adjacent placer localities G3 and G4;(D): comparison of silver contents of eluvial populations G8 and G9 with the adjacent placer population (G10) and a more distal placer sample (G2).

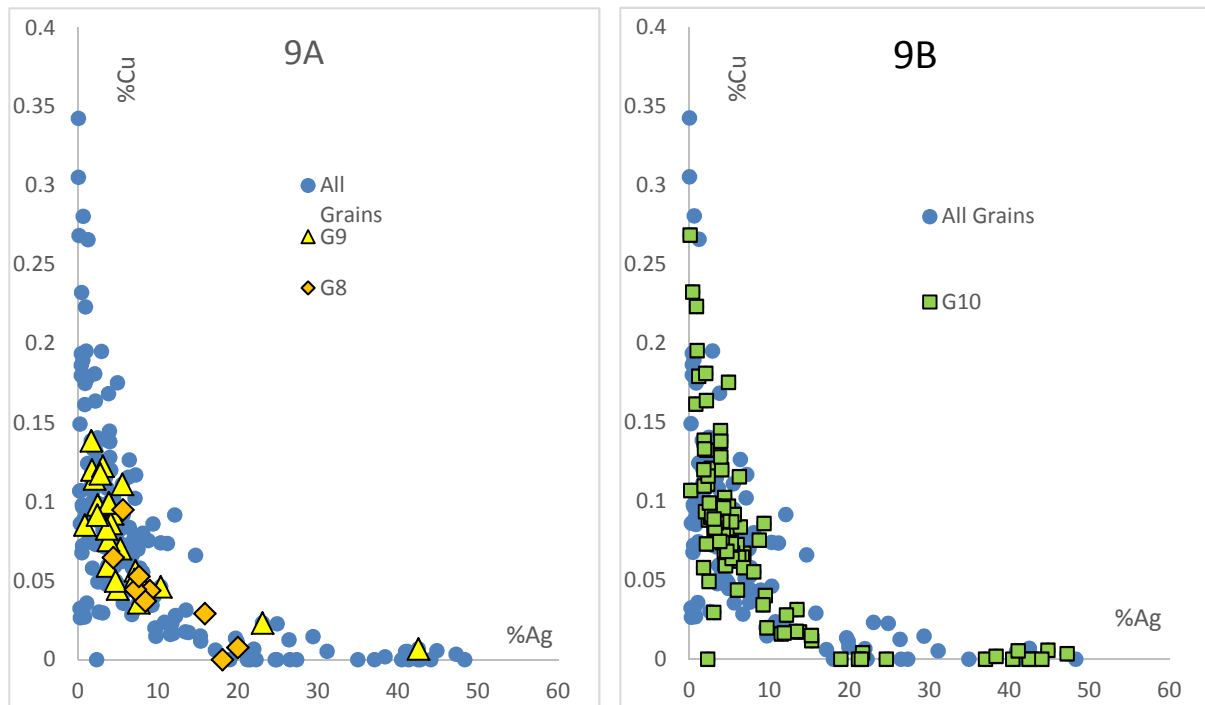


Fig. 9: eluvial environments conform to the high Cu field, but a small number do occur within the high Ag field. A similar approach to the gold grains from the adjacent placer sample (G10) has been undertaken in Figure 9B, but here the full range of compositions is represented.

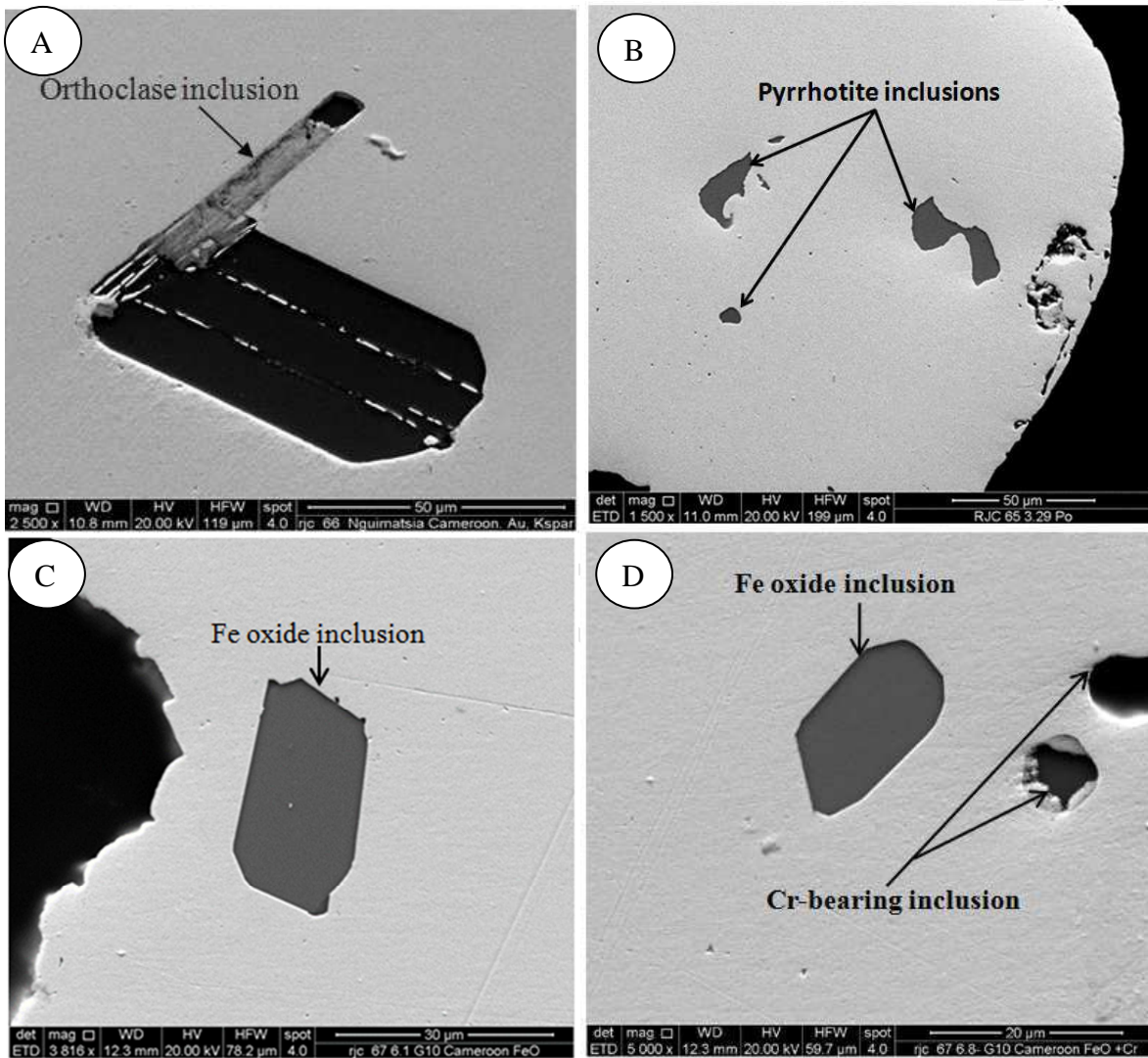


Fig.10: Back-scattered Electron (BSE) images of typical inclusions in placer gold grains. (A) Orthoclase inclusion in-filled by Au alloy in gold grain. (B) Pyrrhotite in detrital grain. (C) Typical Fe oxide inclusion in eluvial gold grain; homogeneity does not suggest alteration from pyrite. (D) Representative Fe oxide containing about 5% of Cr.

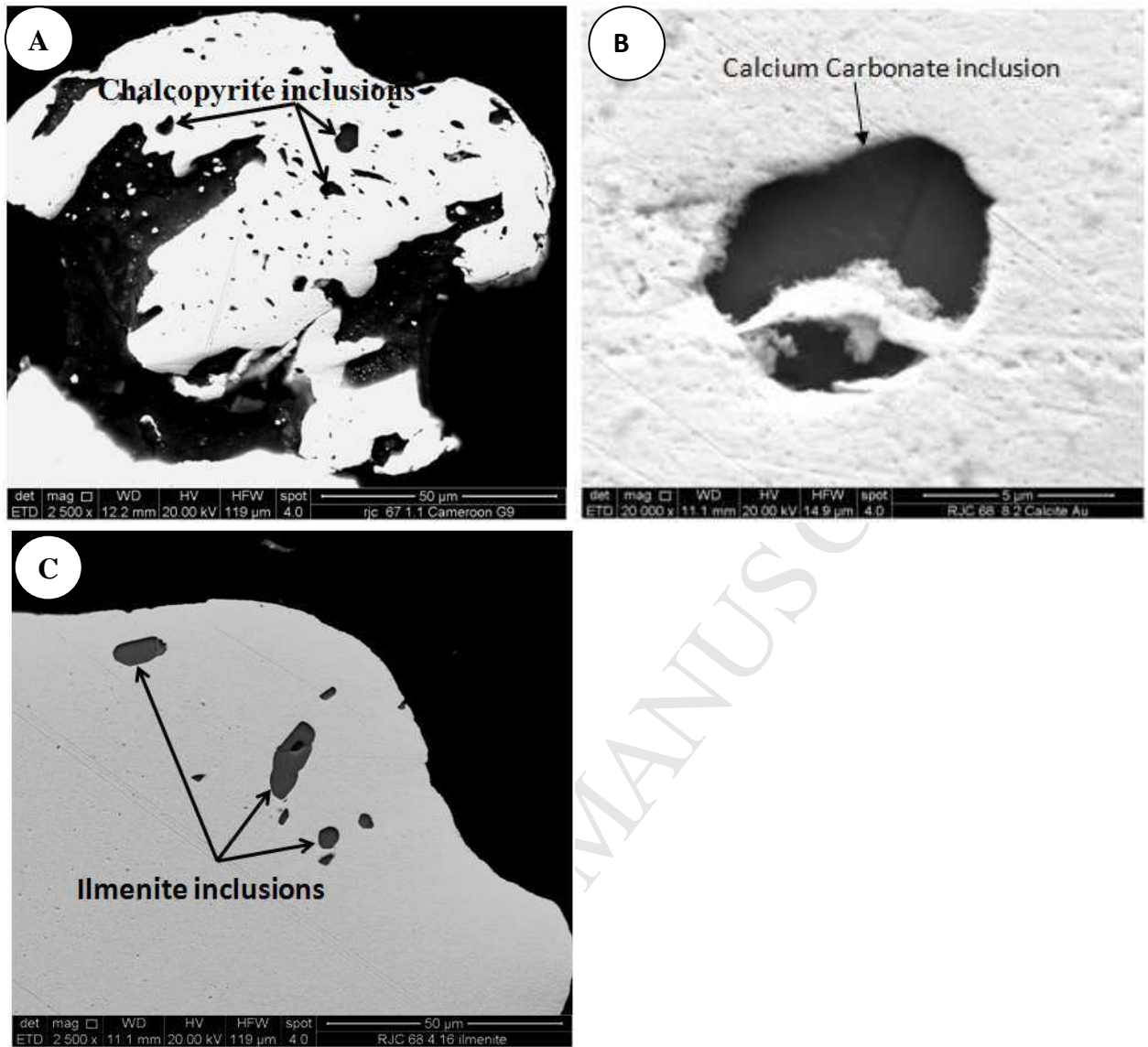


Fig.11: Back-scattered Electron (BSE) images of some silicate, carbonate and oxide inclusions of placer gold grains. (A) Chalcopyrite inclusions in gold grain. (B) Calcium carbonate inclusion in gold grain from site G7. The calcium carbonate grain is bridged by secondary Au which postdates it. (C) Ilmenite inclusions in gold grain from site G4.

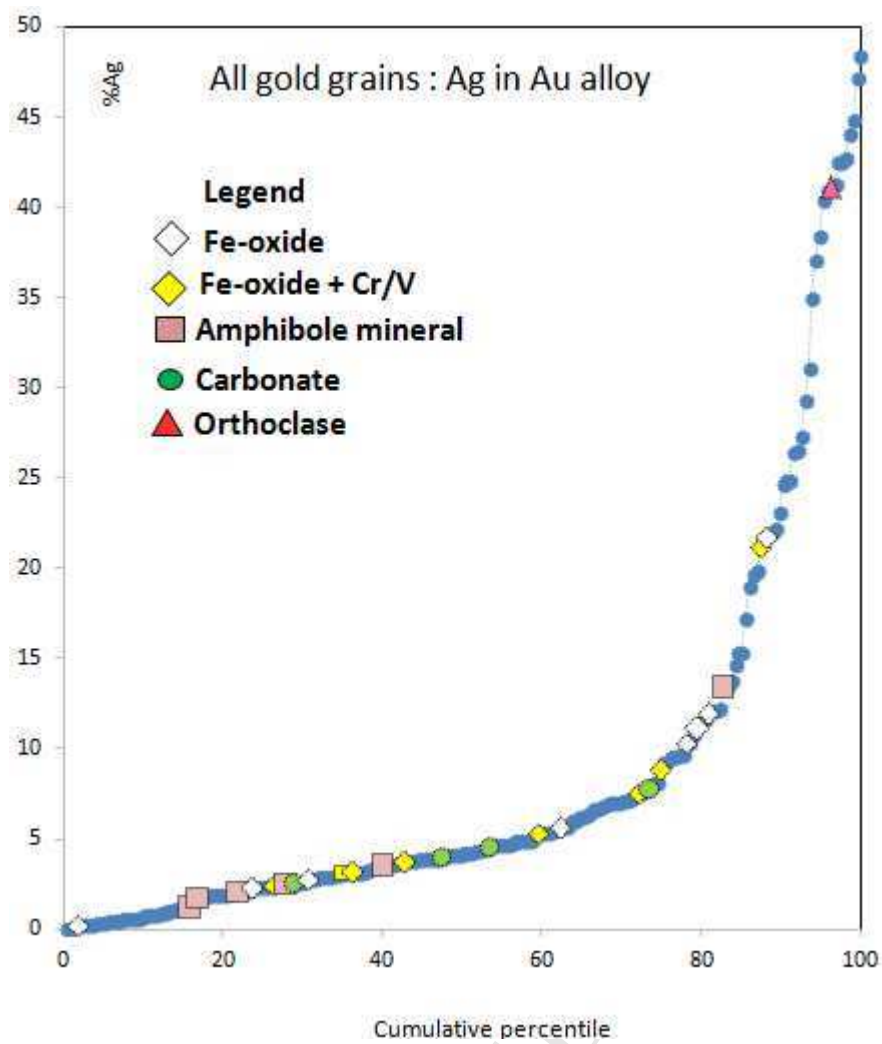


Figure 12: Relationship between inclusion species and host alloy.

Highlights

Morphologically, placer gold grains show a wide variety of shapes, but the fragile crystalline form and pristine faces on most eluvial grains provides evidence of very limited transport and therefore a restricted local source.

Although the in-situ sources of these gold particles remains unknown, a secondary origin may be discounted because of the mineralogy of the inclusion suite.

The gold alloy composition is predominantly a binary Au-Ag alloy with minor contributions from Cu. Magnetite inclusions, sometimes containing Cr and V, are common and suggest a relationship between gold mineralization and local amphibolite.